Determining the Root Causes of Excess Metal and Void Defects With Respect to the Photoresist Quality in Thin Film PZT Fabrication Processes

by

Jun Bum Lee

B.S in Mechanical Engineering, University of Illinois at Urbana-Champaign 2011

Submitted to the Department of Mechanical Engineering
in partial fulfillment of the requirements for the degree of

Master of Engineering in Manufacturing

at the

MASSACHUSETTS INSTITUTE OF TECHNOLOGY

August 2012

Author .....

Jun Bum Lee
Department of Mechanical Engineering
August 10 2012

Certified by .....

Jung-Hoon Chun
Professor of Mechanical Engineering
Thesis Supervisor

Accepted by .....

David Hardt
Professor of Mechanical Engineering
Chairman, Departmental Committee on Graduate Studies

DISCLAIMER

MISSING PAGE(S)

The abstract is missing from this document. This is the most complete version available.

ACKNOWLEDGEMENTS

First and foremost, I am most indebted to Professor Jung Hoon Chun, who provided us with invaluable advice and support. He always pointed us in the right direction and this thesis would not have been possible without his mentorship.

I'm also very grateful for all the cooperation and interest of Michael, Mike, Eric, Barbra and the rest of the PZT cell. Each and every one of them supported us with enthusiasm and created an environment in which we felt welcomed.

I would also like to extend my gratitude to Professor David Hardt and the director of the program, Dr. Brian Anthony for giving us the opportunity to participate in this exceptional experience.

I would like to express my appreciation for Jennifer Craig who greatly helped me construct this thesis properly. Writing this thesis in the given schedule would have been exceedingly more difficult had Jennifer not truly cared about my, and the rest of the program's, success.

It has been the greatest pleasure to have worked with my teammates Neha Dave and Abdulelah Alsaeed. It was the best team I have had the chance to work with by far.

I would also like to thank my parents who never once doubted me throughout my years in college. They were my motivation and strength, which always pulled me through.

Last but not least, I wish to thank my beloved Anna Lee for her perpetual support. Her patience and understanding were far beyond what I could ever have asked for.

TABLE OF CONTENTS

LIST OF FIGURES

LIST OF TABLES

CHAPTER 1

INTRODUCTION

1.1. Motivation

This project is based on data and processes from a company specializing in volume production of lead zirconate titanate (PZT) thin film devices. These PZT substrates are used to manufacture a variety of products in a cleanroom-like environment. The product line of interest in particular, consists of a small ceramic substrate with wiring printed onto the surface in specific, predetermined pattern. When electricity is passed through, the PZT substrate actuates differently based on which circuit the electricity supplied to. Hence, it is important that these circuits are printed precisely as any type of shortage or leakage of current can cause the devices to malfunction. Therefore, high quality devices must not have any surface or material defects.

Currently, the total of approximately fifteen percent of devices are rejected for excess metal defects, holes or voids in the pattern, or cracks and breaks in the ceramic material. Since each rejected device results in wasted material, labor time and cost, any reduction in the occurrence of these various types of defects will directly correspond to an increase in revenues for the company. Figure 1.1 shows a detailed breakdown of each type of defect's contribution to the reduction of total yield.

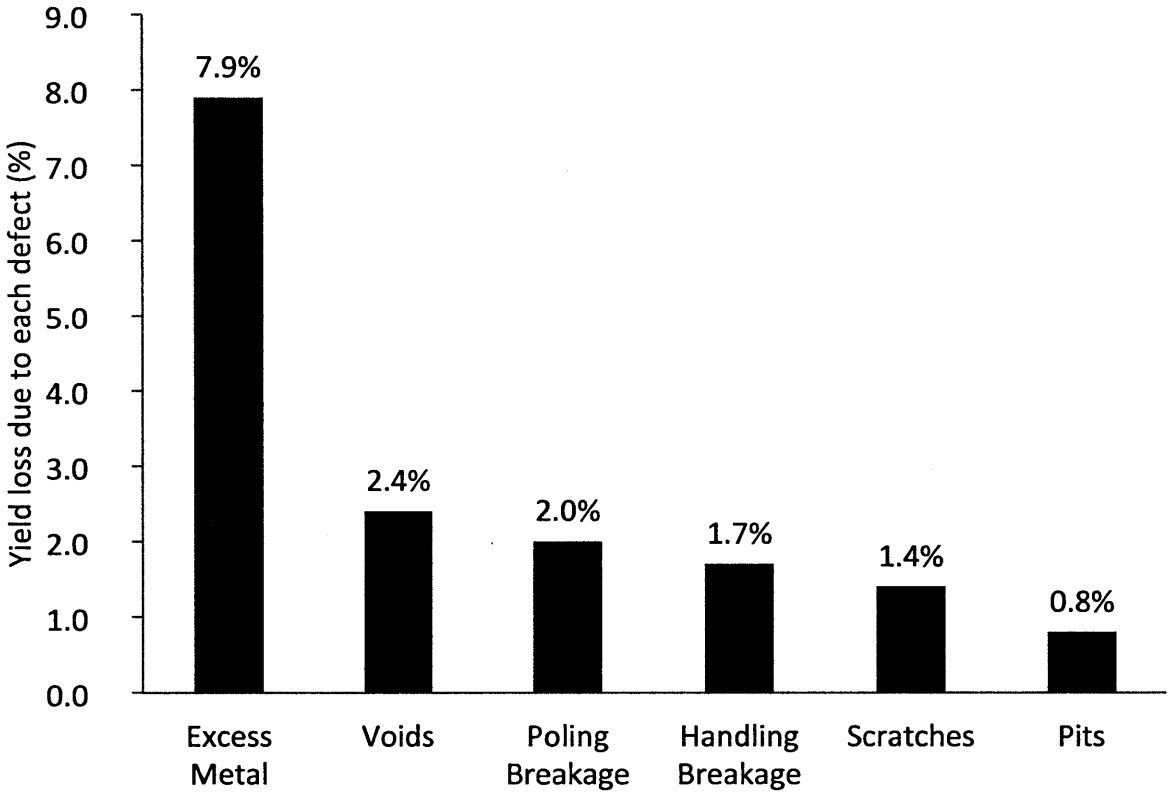

Figure 1.1: Primary defects and their corresponding yield loss percentage in 2011. Excess metal contributes most significantly, followed by breakages and voids.

1.2. Process Overview

It is helpful to grasp an overview of the manufacturing process in order to better understand the project focus as well as the objectives. This section will briefly describe the processes that a PZT substrate undergoes. Figure 1.2 outlines this high volume manufacturing process, as well as the basic function and primary source of yield loss at each stage.

The manufacturing process for PZT is initiated by coating the substrates, or ceramic wafers, with their metal layers. First, a single barrier layer of WTi (WTi) is deposited across the entire surface of the PZT substrate to promote the adhesion between the substrate and the subsequent Ni (Ni) layer. The coated substrate is then sputtered with a layer of Ni, which is intended to carry current through the device. The material then undergoes a process called poling, which will change its molecular orientation to enhance its inherent piezoelectric properties.

The patterning process follows. First, the metalized substrates are sprayed with a protective photoresist layer. A mask with an image of the pattern is then placed on top of each substrate, which is then exposed to a flood of high intensity Ultraviolet (UV) light. Any photoresist that was not shielded by the mask from the UV light will dissolve in the developing bath, leaving behind a pattern of intact photoresist in the shape of the circuit wiring. A wet etch process is then performed to remove metal in the non-patterned areas. The process of coating, exposing, developing and etching these substrates is collectively known as photolithography. At the end of the photolithography stage, the devices are electrically functional but still connected to each other on the substrate. To separate them, the substrates are diced into individual devices for final testing and application.

Throughout the manufacturing process, a number of visual and electrical quality inspections take place to quickly identify process control concerns. Reject devices are typically eliminated in the final inspection stage. Once the operators have verified the electrical and visual quality of all devices, they are carefully packaged and sent to the customers.

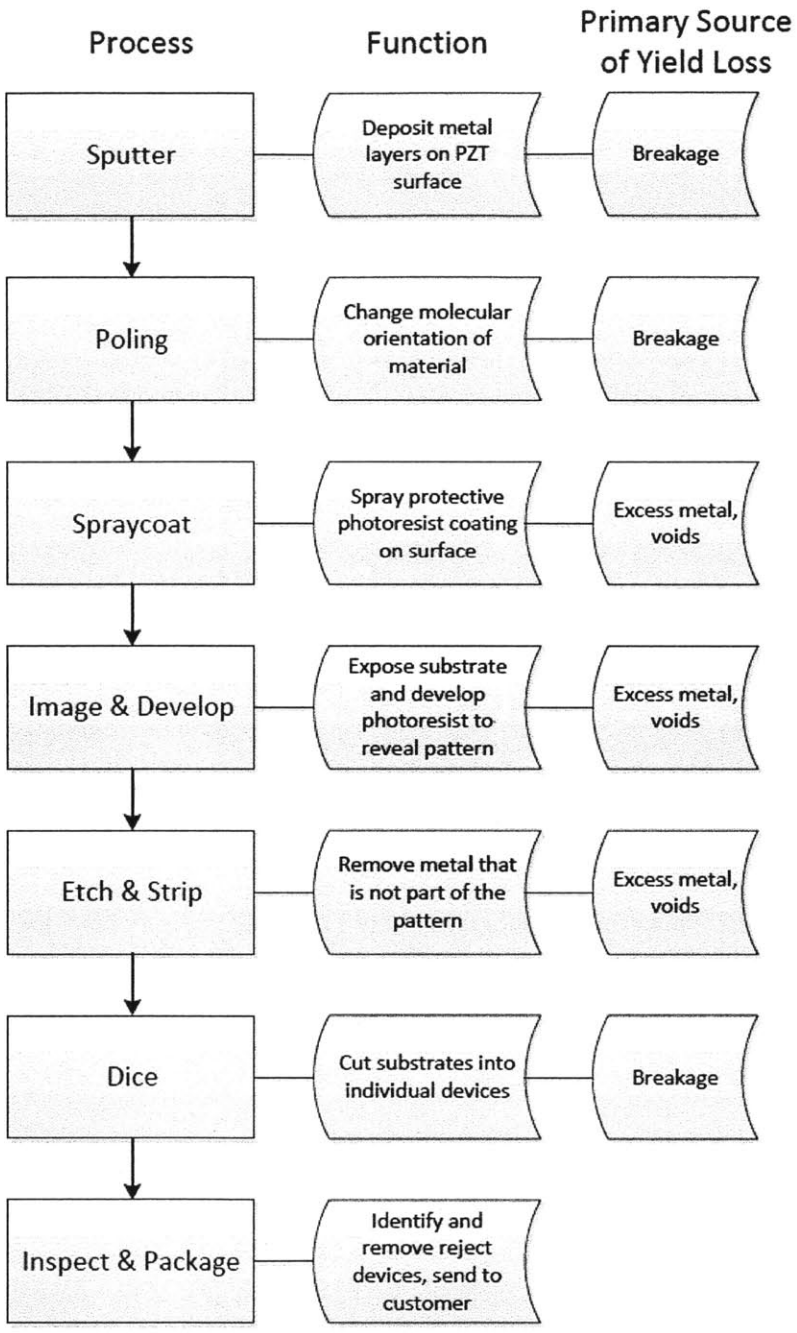

Figure 1.2: Outline of manufacturing process for PZT thin films.

1.3. Objectives

The principal objective of this project is to identify and eliminate the causes of defects with significant contribution to yield loss, thereby increasing the manufacturing yield. In order to achieve this improvement, the project was divided into three separate tasks, each established to target a leading cause of defective devices. These tasks are listed below:

- Determine the root causes of excess metal and void defects with respect to the quality of the spray photoresist.
- Eliminate excess metal defects due to incomplete metal and oxide removal.
- Eliminate breakage due to the poling process.

This thesis, in particular, will focus on determining the root cause of excess metal and voids. As the defects in the photoresist has been suspected as the primary cause of excess metal and void defects by the company, the subsequent analysis was focused on the photoresist defects that could lead to final device defects. The specific objectives of this thesis:

- Verify that excess metal and void defects are end products of photoresist defects.
- Identify during which process and why these photoresist defects are taking place.

1.4. Task Division

In order to achieve significant manufacturing yield improvements for this company, it was necessary to divide the project and target three individual process steps. This author was responsible for the investigation of the root causes of excess metal and void defects generated from defective photoresist quality, while Neha Dave [1] aimed to reduce these defects as they related to etching. Abdulelah AlSaeed [2] was responsible for the elimination of yield loss due to breakage inside the poling machine. All team members shared the underlying goal of yield improvement.

1.5. Thesis Organization

The overall goal of this thesis is to experimentally verify the various causes of excess metal and void defects. Chapter 1 introduces the challenges and the objectives of this thesis. Chapter 2 describes the photolithography process, both in the general thin film industry as well as the company specific scenarios, and outlines the necessary topics required to better understand the subsequent analysis such as the spray photoresist, exposure, development and baking processes. Chapter 3 explains the analysis of defects conducted in order to confirm the existence of photoresist defects and to determine during which particular photolithograph process these photoresist defects are generated. The effect of particle and fiber contamination is tested and photographed then the sources of these various photoresist defects are outlined. Chapter 4 describes the experimental methodology that was used to test the sources of defects and the results of these experiments are discussed in Chapter 5. Chapter 6 summarizes and suggests a conclusion for experimental results. Lastly, Chapter 7 proposes possible future tasks to further verify the conclusions and recommends process changes.

CHAPTER 2

PHOTORESIST PROCESS BACKGROUND

A degree of understanding in general as well as the company specific photolithograph processes is necessary in order to better comprehend the subsequent analyses. Hence, this chapter will provide a general overview of how and why certain processes are performed in thin-film manufacturing and company-specific scenarios.

2.1. Spray Application of Photoresist Layer

There are many different ways to coat a substrate with photoresist, all with different strengths and limitations. The most well known methods are spin coating, spray coating, dip coating and roller coating. However, because this particular manufacturing line utilizes only spray coating of photoresist, this thesis will place its focus on the spray coating process.

2.1.1. Ultrasonic Spray

Ultrasonic spray is a type of photoresist application method that utilizes a panel of vibrating piezoelectric crystals to create a mist of photoresist droplets typically between 10 μm and 50 μm

in size. These droplets are then carried onto the substrates by stream of air and merge to form a consistent layer of photoresist. The typical vibration frequency of piezoelectric crystals varies from 20 kHz to 180 kHz and these frequencies determine the size of the droplets. The photoresist must be diluted to low viscosity, usually below 20 cSt, for correct spray operation. The spray machine used in this particular manufacturing line sprays the photoresist by sweeping its nozzle across stationary substrates as shown in Figure 2.1. The two-axis path that the nozzle travels is described by the dotted line [3].

2.1.2. Parameters of Ultrasonic Spray Machine

An ultrasonic spray machine has many parameters that can affect the final quality of the photoresist layer. The evenness of spread and the thickness of the photoresist depend on the following parameters.

- **Scan speed:** Scan speed is the speed at which the nozzle travels along the path. Slower scan speed means more photoresist volume is deposited due to increased time at each nozzle location
- **Flow rate:** Flow rate is the amount of photoresist sprayed per given period of time, often given in the unit of $\mu l/s$. A syringe that compresses at a consistent rate controls the flow rate.
- **Overlap space:** The nozzle sprays photoresist as it travels along its path. As a result, only a small area directly under the nozzle gets the full coat and the density of photoresist gets thinner as the distance increases from the center of spray. Hence, a degree of overlap between the spray areas is required for an even surface to be achieved. Overlap space is measured by the distance of the center of spray from one pass to another as shown in Figure 2.1.
- **Head height:** Head height defines the distance between the substrate and the nozzle head. As the nozzle gets further away from the substrate, the spread of photoresist becomes larger and the number of droplets that actually gets deposited on the substrate decreases. Therefore the head height must remain small, but large enough to avoid turbulence and splashing. Furthermore, large head height forces the droplets to travel for

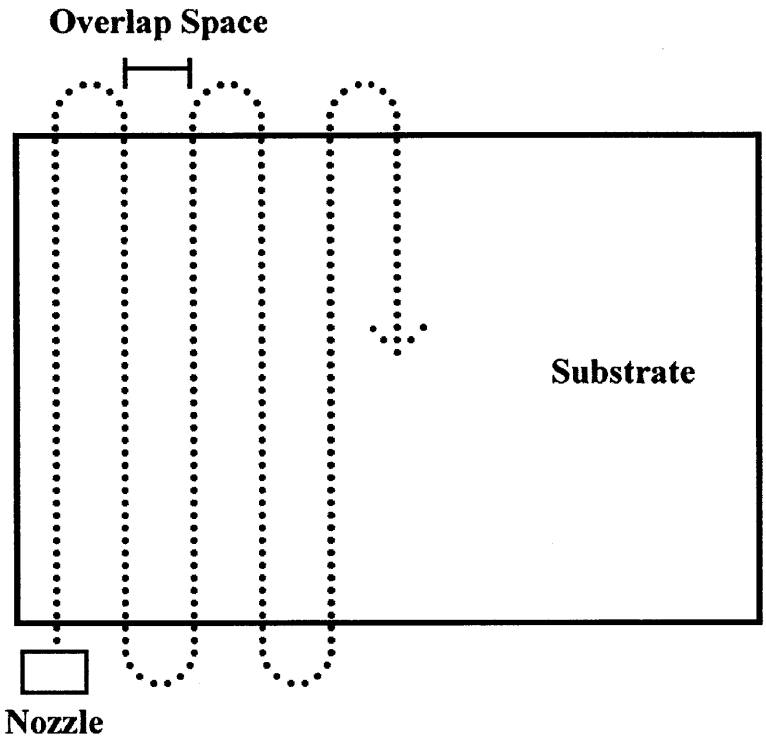

Figure 2.1: Schematics of nozzle path as it sprays a rectangular substrate.

a longer period of time in the air before reaching the substrates. As a result, the amount of solvent evaporation and the droplet viscosity increases.

- **Ultrasonic nozzle head vibrating frequency:** The effect of viscosity will be discussed in detail in Section 2.1.4
- **Photoresist viscosity:** The effect of viscosity will be discussed in detail in Section 2.1.5 [5].

2.1.3. Spray Photoresist Requirement and Qualifications

Photoresist is a mixture of solid and solvent. The term solid content refers to the mass percentage of solid that a photoresist mixture consists of. As the solid content increases, the photoresist becomes more viscous. Photoresists with different solid content are used for spray operations depending on the desired resist layer thickness and surface roughness. In general, for spray coating, higher solid content is required to create thicker resist layers, but at the cost of increased surface roughness. Photoresist with low solid content, typically below 25% is required to meet the viscosity upper limit of 20 cSt for spray coating processes. The currently utilized photoresist, in this particular manufacturing sequence, contains 22% solid content, which is created by diluting a stock photoresist with a known solid content with additional solvent. It must be noted that a diluted photoresist has shorter shelf life as additional solvent accelerates the aging of the resist and promotes precipitation [3].

2.1.4. The Drop Size and the Photoresist Layer Quality

The size of spray droplets, can have a significant effect on the overall quality of a photoresist layer. Three factors can affect the drop size: the vibrating frequency, surface tension and density. The interaction of these three terms and their effects on the drop size is described by Lang's formula on the number median particle (droplet) diameter [6].

$$d_h = 0.73\sqrt[3]{\frac{T}{\rho f_a^2}} \tag{1}$$

where ρ represents the photoresist density, T is the surface tension and f_a^2 is the atomizer frequency respectively. It should be noted that the actual measurements of droplet size could vary from the calculated values depending on the different measurement techniques and environment conditions [7].

The quality of the photoresist layer is directly affected by the drop sizes. Larger droplets can be associated with various photoresist defects, such as bubble formation, voids and overall uneven surface portfolio. These effects are further investigated in Section 4.4.1 and 4.4.3.

2.1.5. Solid Content and Photoresist Layer Quality

In addition to the size of the droplets, the viscosity of the droplets also affects the photoresist layer quality. Without sufficient solvent content in the photoresist, the droplets cannot effectively flow and merge in order to create an even surface. This effect of wet droplets spreading after reaching the substrate surface is called the flowing effect. The flowing effect increases with the decrease in solid content, which leads to reduction in surface irregularities. A separate study of photoresists with different solid content describes the extreme sensitivity of the surface roughness to the solid content level of the resist. The evenness of the spread was measured by the surface roughness and the result of this study shown in Table 2.1. These experiments were performed using a particular spray machine called EV 101 and polished silicon substrates. As can be seen in Table 1, the surface roughness was reduced by more than one order of magnitude with 3% decrease in the solid content. The downside of reducing the solid content however, is the reduction in maximum film thickness and longer drying time. The study also indicates that 15% solid content photoresist yielded the lowest surface roughness while maintain the 5 μm thickness. The number 15% was utilized in one of the subsequent analysis described in Section 4.4.2 [1].

2.2. Imaging Process of Photoresist Layer

The exposure and development processes that are used to pattern the photoresist are collectively called the imaging process. The photoresist layer protects certain areas of underlying metal layer from being chemically removed in the subsequent etching process. During positive imaging, the

Table 2.1: Sensitivity of the surface roughness to the change in solid content of photoresist [3].

Solid content (%)	17	20
Viscosity (cSt)	10.4	16.9
Roughness (μm)	0.225	2.9

negative areas of the photoresist are exposed to UV light that weakens the photoresist, while the positive area is shadowed from UV light by a photomask. Photomasks are made of glass and positively patterned with chrome. Therefore, they allow the UV light to pass through in the negative while reflecting the light in the positive. The weakened photoresist is chemically removed and creates the resulting pattern that is identical to the photomask. This process is critical as the photoresist pattern is the only layer that protects the metal layer underneath. If any defects develop in the photoresist pattern, the metal layer pattern will mirror that defect.

2.2.1. Wavelength Absorption and Spectral Sensitivity

The majority of modern photoresist contains a photoactive compound group called diazonaphotoquinone (DNQ). This particular compound has the optical absorption spectrum ranging from blue light to UV, which is responsible for the typical reddish-brown or purple color of photoresist. A mercury vapor lamp (Hg light source) is used to generate a flood of UV light that matches the optical absorption spectrum of DNQ in order to trigger the photoreaction. The typical emission spectrum of Hg light sources contains g-line, h-line and i-line, with 436nm, 405nm and 365nm wavelength, respectively. As each photoresist has different absorption spectrum, the amount of exposure required can vary and must be calibrated [8].

2.2.2. The Photo Reaction

The presence of the photoactive compounds DNQ reduces the alkaline solubility of the organic photoresist chemical. However, upon exposure to UV light, DNQ compound decomposes and transforms into carboxylic acid and nitrogen gas in the presence of H_2O. The carboxylic acid is more alkaline soluble then DNQ containing unexposed photoresist. In addition, the increase in chemical diffusibility developed by porous structures from the release of nitrogen further raises the solubility. The alkaline solubility of exposed photoresist increases by several orders of magnitude higher than that of unexposed photoresist depending on the concentration of DNQ compounds. The 'weakened' photoresist is then dissolved in alkaline solution through a process called development, which is discussed in Section 2.3 [9].

2.2.3. 'Thin' and 'Thick' Film Exposures

The depth of exposure light penetration relative to the thickness of the photoresist defines whether the photoresist is thin or thick. The penetration depth varies with the type of photoresist and exposure wavelength used, but the film is defined as "thick" if the film thickness is much larger than the penetration depth of exposure light. In a standard setting with g, h or i-line photoresist and exposure light, the penetration depth is between 1 and 2 μm. As a result, thickness more than 5 μm is typically considered thick while less than 1 μm is considered thin. Since the resist layer thickness of the current process is 6.6 μm, the photoresist is considered thick. For thick films, the exposure light cannot fully penetrate the thick photoresist layer from the beginning. Hence, a unique photoresist property called bleaching is utilized to ensure that the whole depth is exposed. As shown in Figure 2.2, photoresist becomes UV-transparent in other words, bleached, when exposed. Therefore, although only the first 1 to 2μm of the top layer is exposed in the beginning of the process, the exposed depth soon becomes UV-transparent and allows the light to penetrate the 2 to 3 μm regions. The penetration depth grows approximately linearly with the exposure time while the rate depends on the composition of the photoresist and the UV light source intensity [8].

2.2.4. The Photomask and Mask Aligner

In order to hold the photomask in place and shine UV light vertically, a device commonly known as mask aligner is used. The purpose of a mask aligner is to align the photomasks relative to the substrates and hold them in place. By doing so, the patterns are transferred onto the substrates in the identical locations and orientations. Mask aligners are also accompanied by the Hg light source for the exposure process.

2.3. Development of Photoresist

Development is a term used to describe the process of removing the weakened area of photoresist using alkaline solution. Developers can deteriorate both exposed and unexposed photoresist but at different rates. The attacking and removing chemical process of exposed

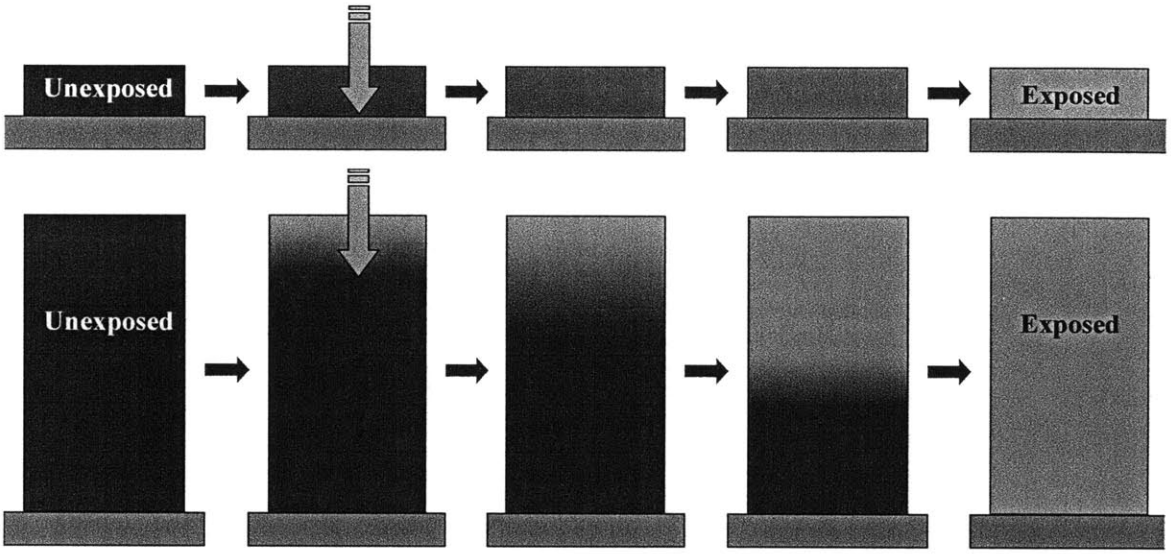

Figure 2.2: Bleaching of photoresist with exposure [8].

photoresist is called development while that of unexposed photoresist is called dark erosion. The rates of both exponentially increase with the developer concentration. Therefore, the optimal dilution level of the solutions, as well as the developing time, must to be experimentally identified as they depend on prior photoresist processes. Ideally, the developer concentration and developing time should be sufficient enough to dissolve all exposed photoresist while minimizing dark erosion of unexposed photoresist.

2.4. Development of Photoresist

Development is a term used to describe the process of removing the weakened area of photoresist using alkaline solution. Developers can deteriorate both exposed and unexposed photoresist but at different rates. The attacking and removing chemical process of exposed photoresist is called development while that of unexposed photoresist is called dark erosion. The rates of both exponentially increase with the developer concentration. Therefore, the optimal dilution level of the solutions as well as the developing time must to be experimentally identified as they depend on prior photoresist processes. Ideally, the developer concentration and developing time should be sufficient enough to dissolve all exposed photoresist while minimizing dark erosion of unexposed photoresist.

2.5. Baking of Photoresist

In between the coating, imaging and etching of the substrates, baking processes can be introduced to enhance the strength and the resolution of the photoresist. Baking processes are meant to reduce the solvent content of the photoresist layer, which provides various advantages.

2.5.1. Oven and Hotplate

There are two ways to bake the substrates coated with photoresist: an oven and a hotplate where the main difference is the mechanism of heat transfer. Photoresist in an oven experiences different effective temperature from that on hot plates due to the presence of large temperature variations inside an oven inherent to convection heat transfer as opposed to conduction. Hence,

baking to reduce solvent content requires more time and a higher temperature than with a hot plate. Due to the lack of direct contact with a conductive surface, photoresist in a typical oven often requires at least 10 minutes to reach the desired temperature. Furthermore, it is experimentally verified that there are 5°C to 15°C of temperature differences inside the current baking oven chamber. Therefore, utilizing a hot plate can provide shorter bake time and a more consistent result between the substrates. However, these disadvantages can be outweighed by in a large scale manufacturing scene where the accuracy and the length of bake time are not critical and simultaneous baking of multiple substrates can be advantageous [10].

2.5.2. Softbake

Reducing the solvent content after coating the substrates has a number of effects that help minimize defect formation during exposure and developing.

- Improved adhesion of the photoresist layer to the substrates.
- Prevention of sticking and contamination of the photomask during exposure as the photoresist becomes harder following the reduction of solvent.
- Prevention of nitrogen bubble formation inside the photoresist from high solvent content.
- Reduction of dark erosion during development [10].

2.5.3. Consequences of Under/Over Softbake

Softbaking thick photoresist layers for longer or shorter than optimal duration can result in various undesirable outcomes. If a thick photoresist is not softbaked sufficiently due to a too low temperature or for too short of a period, bubbles can form and dark erosion rate increase. Although photoresist outside the pattern area is not directly exposed to the UV light, nitrogen bubbles can form at the edges of the pattern and deteriorate the pattern resolution. Also, a high concentration of solvent can accelerate the erosion of unexposed photoresist, creating voids or chips. On the other hand, baking in a high temperature oven or baking for too long can partially decompose the photoactive compounds and decrease the development rate and increase the

exposure time required. Extended exposure and development can damage the resolution of the pattern [10].

2.5.4. Hardbake

After imaging of the softbaked photoresist, an additional bake step can be introduced to increase the thermal, chemical and physical stability of the photoresist structure. A process during which a substrate with imaged photoresist is baked commonly between 110°C and 150°C is called hardbaking. As a result, the remaining solvent content of the photoresist is evaporated and the chemical and thermal stability of the photoresist is increased. Hardbaking is often required to protect the photoresist from deterioration during aggressive chemical processes such as wet etching, dry etching, and electroplating. An insufficient hardbake process can lead to loss in pattern resolution, dimensional inaccuracy and voids in the underlying metal layer. The solvent content is typically between 3% and 5% after softbake and approaches 0% after hardbake. In addition, hardbake also mechanically relaxes the photoresist through a phenomenon called reflow, as described in section 2.55. Reflowing allows higher photoresist adhesion to the substrate surface and prevents pattern undercuts.

The photoresist begins to thermally cross-link at elevated temperatures approximately 140°C, at which the photoresist and underlying substrate molecules start to bond. In addition to the reduction of solvent content, thermal cross-linking increases the stability of the resist and helps the resist withstand the etchants. A hardbaking step is often redundant, but sometimes inevitable for subsequent processes with harsh chemical attack such as nitric acid etching [11].

2.5.5. Reflow of photoresist

All types of photoresist that are cross-linked have a softening point at which the resist will undergo thermal softening and rounding. This effect of reflow can be undesirable as it may interfere with dimensional accuracies; however, it is inevitable during hardbake as the softening temperature is generally between 100°C and 130°C. In this temperature range, the contact

between the resist and substrate remains unaffected while the upper edges of the pattern become round as described by Figure 2.3 [12].

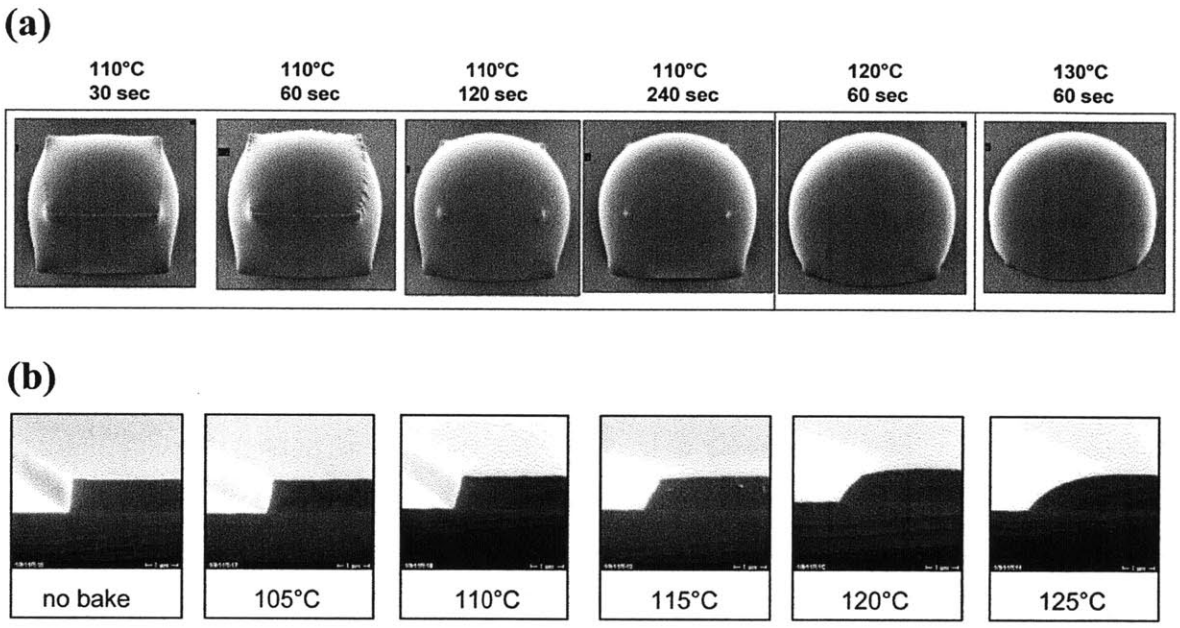

Figure 2.3: Reflow of 80 AZ 40XT cubes at different temperature (a) and rounding of the upper edges with reflow (b) [12].

CHAPTER 3

ANALYSIS OF DEFECTS DURING PHOTOLITHOGRAPHY

An analysis of defects was conducted in order to confirm the existence of photoresist defects and which aspects of these defects were causing excess metals and voids. The result of the analyses showed that the imperfect photoresist quality is present and is responsible for both the excess metal and void defects. The contamination and imperfect coverage of the photoresist were identified as the primary contributors of excess metal and voids and, therefore, their various modes of formation were outlined. This chapter explains in detail how the defect analyses were conducted and explains the potential sources of defects. In order to do so, it is important to first understand the definitions of the terms 'excess metal' and 'void' defects.

3.1. Definition of Excess Metal

Excess metal is a term that is used to describe the presence of any unwanted metal. The presence of metal in areas without circuitry can cause various types of malfunctions in the final device such as current arcing or direct circuit shorting. These types of malfunctions can occur regardless of the excess metal size. Therefore, even the smallest defects must be accounted for. The

phenomenon of arcing can be described with Figure 3.1, in which black color represents the metalized area and white the substrate area. As Figure 3.1 shows, the excess metal particle sits in between the two metal surfaces (1) and (2) and the separation is sufficient so that current will not jump or arc from one surface to another under the highest device operating voltage. However, the probability of current arcing is greatly amplified when a new metalized surface is introduced in between (1) and (2), which effectively reduces the arching distance. As a result excess metal defects can increase the chance of shortage and affect the performance although there is no direct bridging of the two surfaces.

For more detailed defect classification, excess metal defects were organized according to shape, composition and size, as shown in Figure 3.2. The frequency of their appearances was also measured and is represented in the percentage value.

In the classifications provided on Figure 3.2, the droplet and speckling excess metal defects are induced by low photoresist quality while the faded excess metal defects are induced by insufficient etching. Because this thesis concentrates on determining the root cause of excess metal with respect to the photoresist quality, the droplet and speckling excess metal defects were primarily studied.

3.2. Definition of Void

Voids are the opposite of excess metal, in which there are areas of no metal on the circuit. These defects can simply destroy the connecting circuits and create disturbances in the current that can lead to malfunctioning of the device. The primary cause of a void is the insufficient protection provided by the photoresist, either from the lack of coverage or strength to withstand the aggressive chemical attack from etchants. Even a very small gap in the photoresist can create a large void defect if the etchant is allowed to smear in and dissolve the metal. Typical types of voids are described in Figure 3.3 and Figure 3.4.

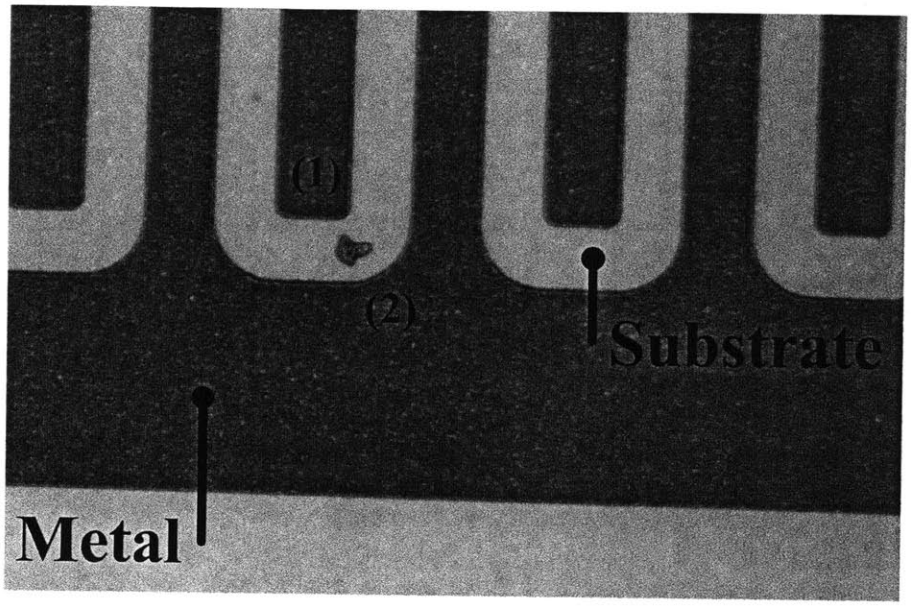

Figure 3.1: Description of excess metal arcing. The excess metal that lies between the point (1) and (2) may allow the current to jump across.

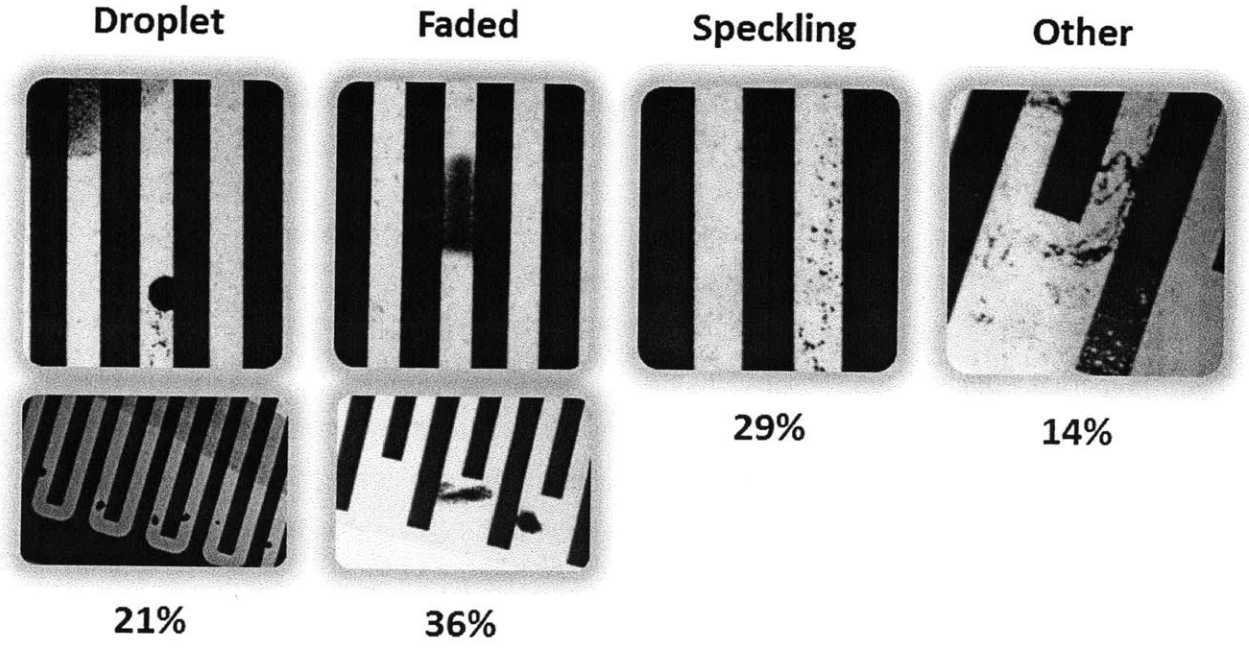

Figure 3.2: Excess metal classification.

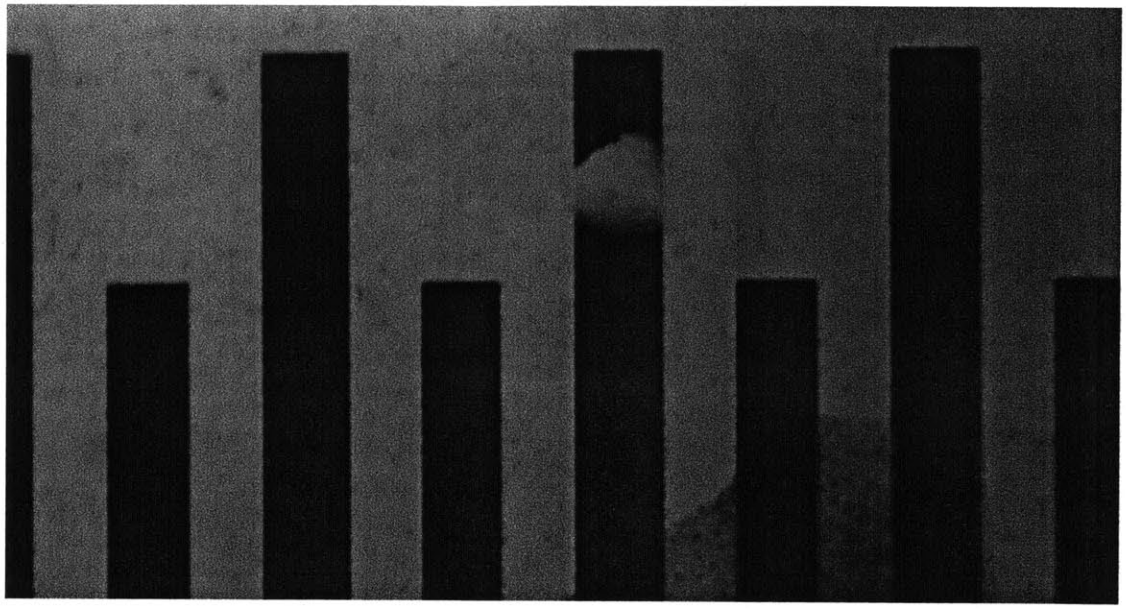

Figure 3.3: Example of void defect 1. The black pattern is the metal and the background is the PZT substrate. As can be seen, the void defect completely cuts off the circuit.

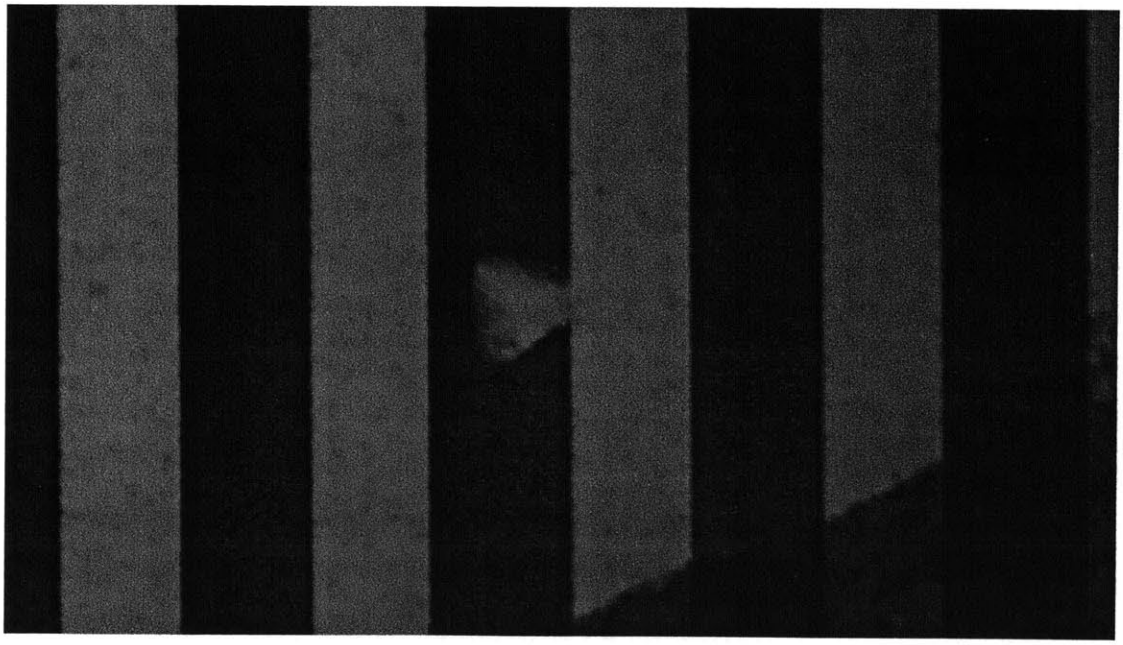

Figure 3.4: Example of void defect 2. The void defect cuts off more than 50% of the circuit width.

3.3. Excess Metal Mapping Test

3.3.1. Overview

A mapping test was conducted in order to investigate which aspect of the bad photoresist quality was causing excess metal defects. The result of this test showed that the particle and fiber contamination of the photoresist were largely responsible for creating excess metal defects.

Various types of defects can be observed on substrates covered with photoresist. Scratches that can be either on the raw material or metal surface look white in color while smudges in the metal layer look black through the light purple color of the photoresist. However, contamination defects in the photoresist are the most easily identifiable as the photoresist bulges around the contaminants. On the other hand, voids in the photoresist are the least identifiable as voids cannot be seen until the photoresist layer is viewed at an angle.

3.3.2. Experimental Methodology

The excess metal mapping test started with metalized and photoresist sprayed substrates. The substrates were first carefully inspected and all defects including particle defects and smudge defects were mapped on the transparencies. Once all of the defects were mapped, the substrates were flood-exposed without the mask, therefore, no pattern, developed then etched. By doing so, only excess metal defects were left on the PZT surface and those defects could be easily detected by viewing the substrates through a backlight. A backlight highlights the presence of excess metal defects by showing them as black spots against the yellow PZT background. The setup of a backlight is shown in Figure 3.5. Location and shape of each excess metal defect was then compared to the previously mapped transparencies in order to investigate what type and size of original photoresist defects actually caused the access metal. If excess metal defects appeared in locations that were not in the original map, the causes of the defects were either too difficult to be visually detected or emerged mid-process. The flow chart of the excess metal mapping process is shown in Figure 3.6.

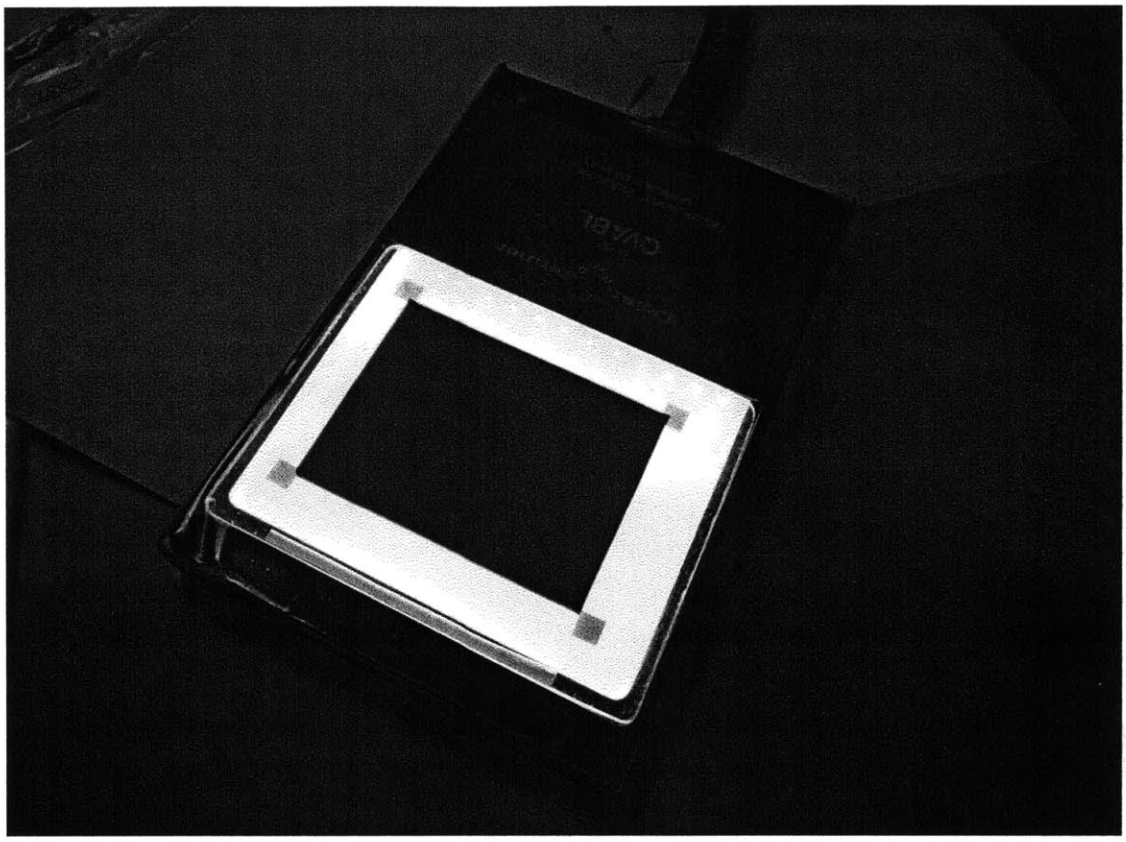

Figure 3.5: The backlight used in the manufacturing floor. The metal blocks the light and looks black under a microscope.

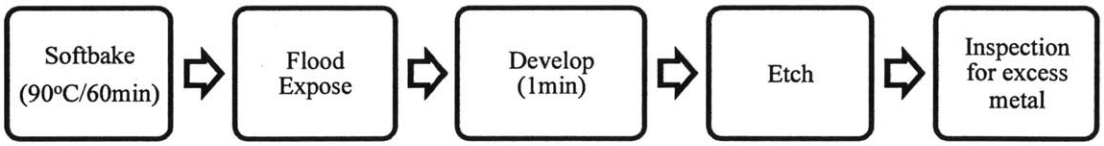

Figure 3.6: Flow chart of excess metal mapping process.

3.3.3. Result

A pair of the excess metal test result is shown in Figure 3.7, where the photoresist defects are marked with blue dots while the final excess metal defects on the substrates are marked with green circles. The summary of all tests carried out on 14 substrates is shown in Table 3.1.

As can be seen from Figure 3.7 and Table 3.1, not all particle and fiber defects in the photoresist layer become excess metals and some new final defects were detected in areas where there were no photoresist defects. In addition, the test confirmed that particles that exceeded approximately 30 μm in size directly left behind excess metal defects shown by the 15 photoresist defects that matched the final excess metal defect locations. The size was estimated from the fact that the line width between the two metal surfaces such as (1) to (2) in Figure 3.1 is 127 μm. Therefore, it was concluded that the particle and fiber contamination of the photoresist was one of the primary contributors of excess metal defects.

3.4. Particle Free Photoresist Substrate Test

3.4.1. Overview

The effect of the particle and fiber contamination of the photoresist layer on excess metal formation was further investigated through a particle free substrate test. The result of this test reinforced the excess metal mapping test in section 3.1 by showing that photoresists with no visible contamination yielded less excess metal rejects.

3.4.2. Experimental Methodology

The particle free photoresist test involved handpicking and creating custom work orders out of substrates with particle and fiber contamination free photoresist. One work order consists of 14 substrates and each substrate consists of 7 devices. These work orders were then processed through the normal manufacturing line mingled with other normal work orders. It was important to not mark these work orders as experimental, as marked items usually are treated with special

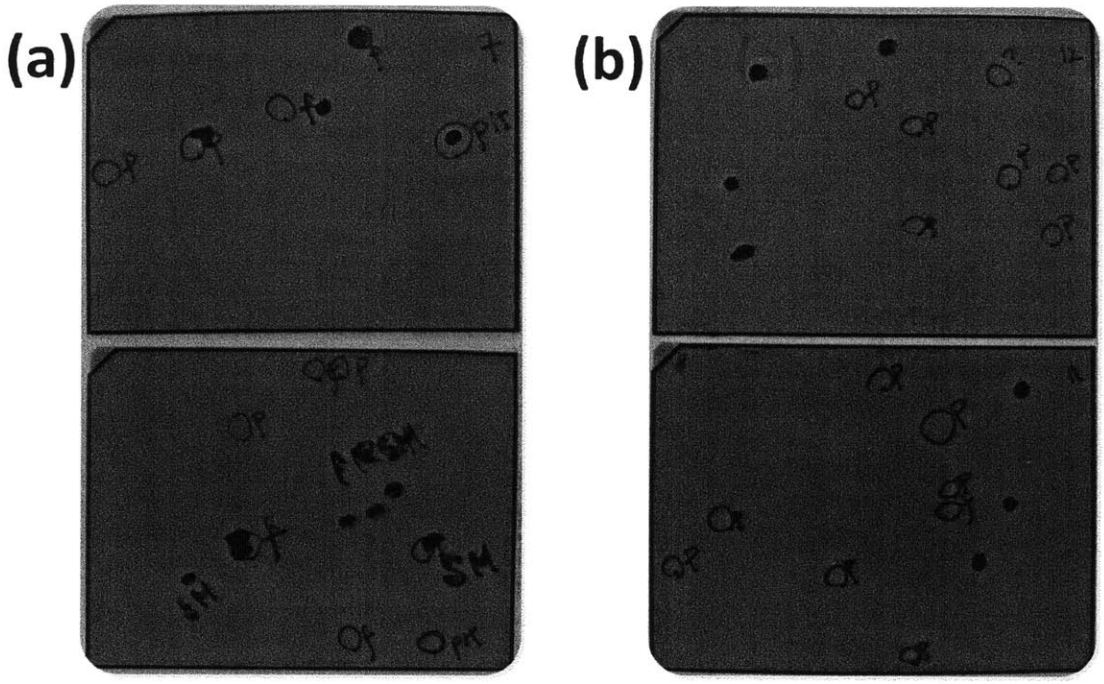

Figure 3.7: Examples of good matches between the photoresist defects and final excess metal (a) and bad matches (b). The blue dots represent the visible defects in the photoresist layer while the green circles represent the excess metal defects after the test processes. Overlapping of these two means that the photoresist defect caused the excess metal defect.

Table 3.1: Summary of the excess metal mapping test. Overlapping defects refer to the number of green circles and blue dots that overlap therefore, showing that photoresist defects induces excess metal.

Substrate Number	Mapped Particles	Excess Metal Defects		Overlapping Defects
		Particles	Fibers	
1	7	4	2	2
2	3	2	0	0
3	4	3	3	1
4	2	2	0	1
5	3	2	5	1
6	2	3	0	2
7	4	4	1	3
8	3	5	2	0
9	2	5	0	1
10	3	10	2	0
11	4	7	1	2
12	3	5	1	1
13	1	5	3	1
14	1	3	0	0
Total	42	60	20	15

care and yield better results. The total excess metal count of four high quality photoresist work orders at the final inspection is shown in Table 3.2.

3.4.4. Result

As shown in Table 3.2, there is a clear reduction in the number of rejects due to excess metal defect when contamination free photoresists are used. The result of this test reinforced the conclusion drawn from the excess metal mapping test in section 3.1 by proving the effectiveness of reducing the number of photoresist contamination in decreasing the excess metal defects.

Substrates with contamination defects were selected from the production line and were observed with high magnification microscopes in order to confirm the shapes of particles and fibers underneath the photoresist. The pictures of these samples are shown in Figure 3.8 to 3.11.

As a result of the two excess metal defect analyses, the subsequent experiments focused on reducing the photoresist contamination.

3.5. Potential Sources of Excess Metal Defects through Photoresist Contamination

Throughout the entire manufacturing process, the contamination can occur in three different processes: the resist mixing, resist spraying and imaging processes. Fibers and particles can be mixed with the photoresist during the mixing process while these contaminants can get on the wet resist inside the spray chamber. Also, the particles can precipitate on the mask or the substrates and shadow the UV light during the imaging process. This section describes in detail how the photoresist can be contaminated from these three processes. Figure 3.12 summarizes the sources of the contamination according to the respective manufacturing processes. Due to the fact that the substrates are subjected to alcohol cleaning and nitrogen blow prior to being sprayed, it was assumed in this analysis that the substrate surfaces are clean at the point of the spray process.

Table 3.2: Handpicked particle/fiber free photoresist work orders. The numbers of rejects are out of 98 devices.

Work order	Total Excess Metal in Rejects	2012 Average
1	2	4.3
2	1	
3	1	
4	1	

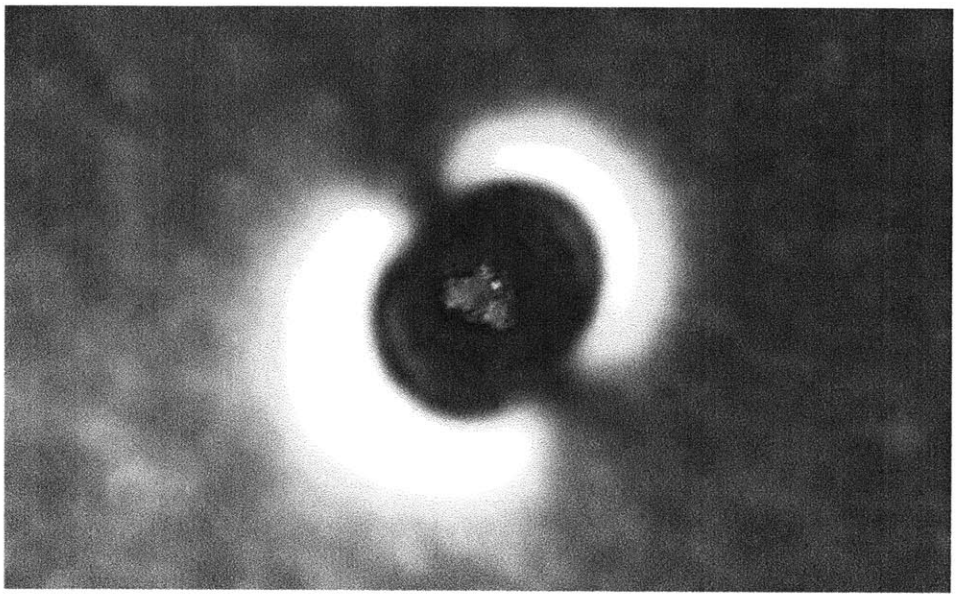

Figure 3.8: High magnification photo of a particle defect in the photoresist layer 1.

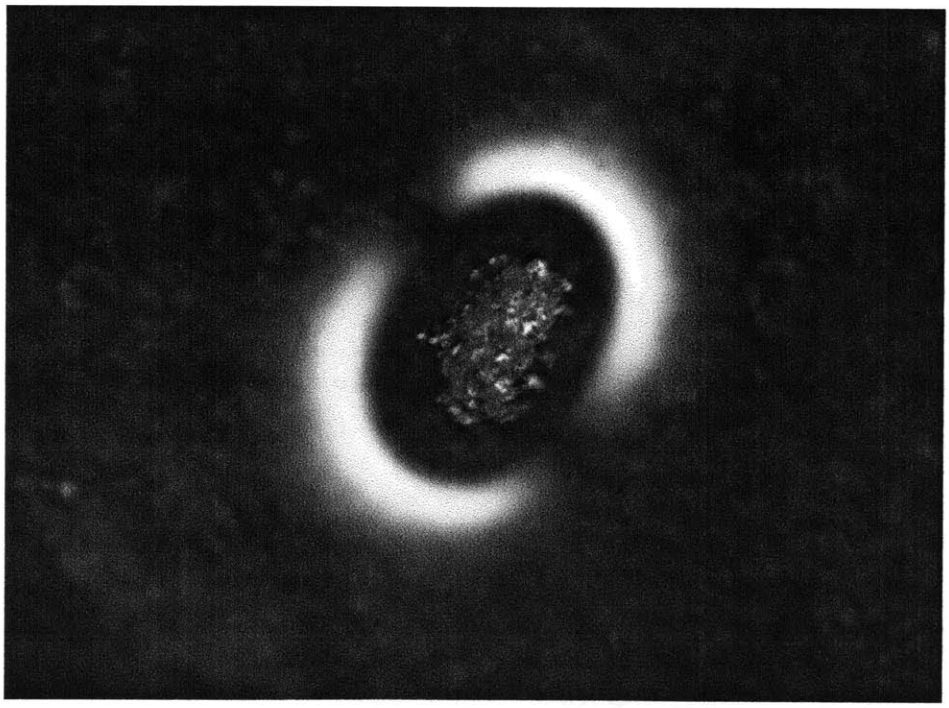

Figure 3.9: High magnification photo of a particle defect in the photoresist layer 2.

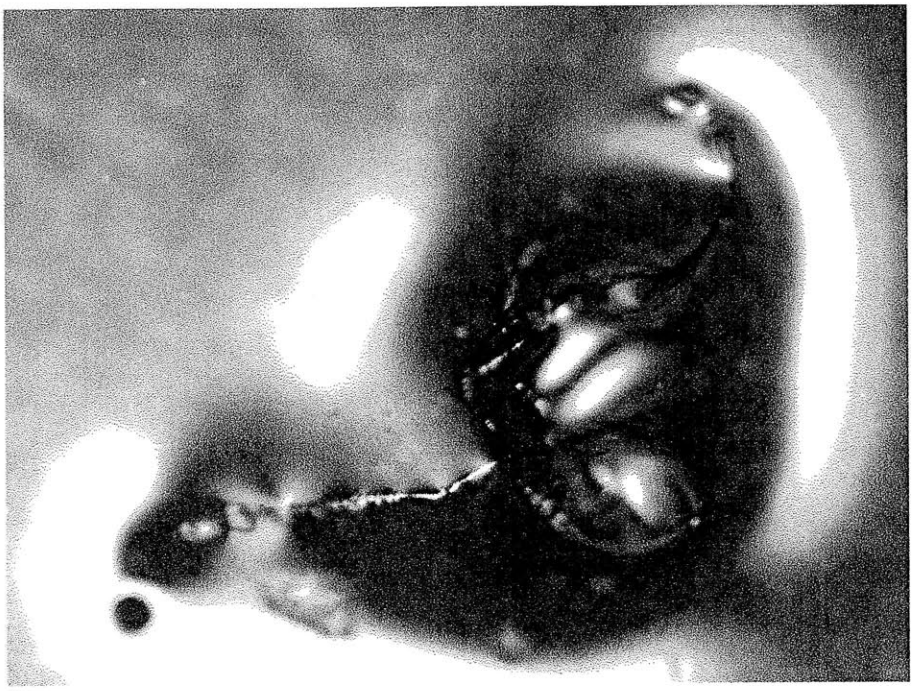

Figure 3.10: High magnification photo of a fiber defect in the photoresist layer 1.

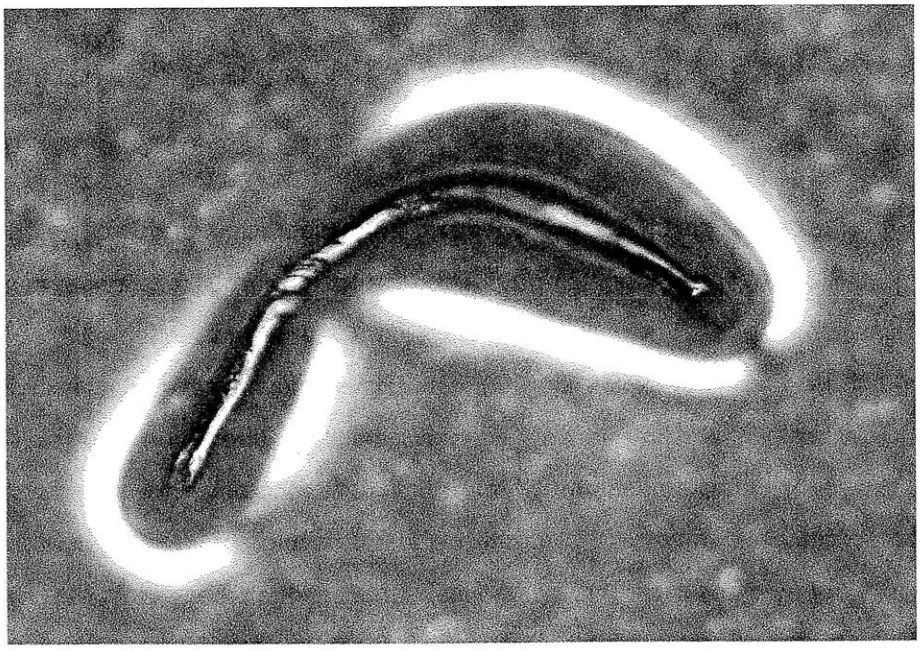

Figure 3.11: High magnification photo of a fiber defect in the photoresist layer 2.

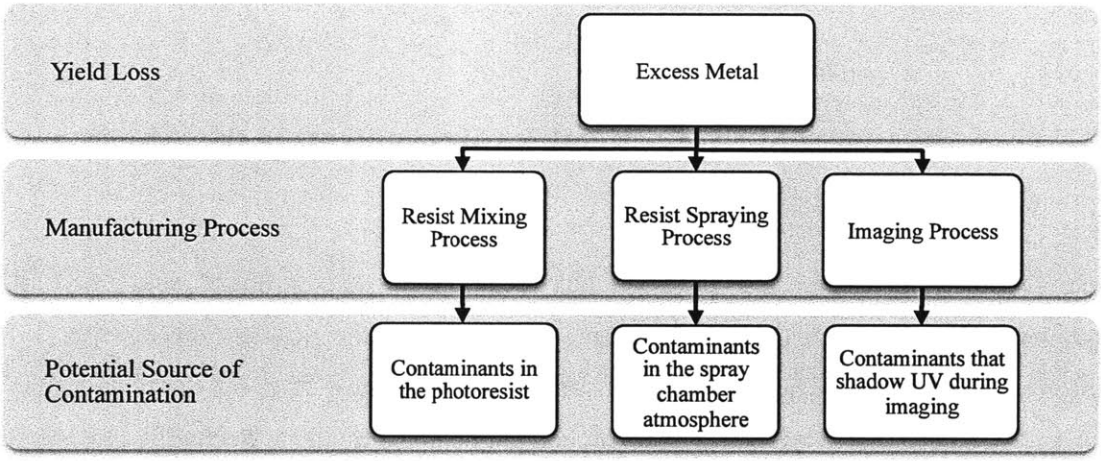

Figure 3.12: Summarized chart of sources of excess metal according to their respective manufacturing process.

3.5.1. Potential Source of Excess Metal 1: Contaminants in the Photoresist

Particles can be introduced into the photoresist during the photoresist and solvent mixing process. Currently, the photoresist is mixed in a negatively pressurized hood with an open top beaker with a magnetic stirrer. Naturally, the photoresist is highly susceptible to contamination from particles and fibers that are present in the atmosphere. Furthermore, the photoresist in the spray machine is unrefrigerated and is of high solvent concentration. Photoresist in such a state is much more susceptible to degradation and form solid precipitates within the photoresist. These particles, fibers and precipitates mixed in the photoresist can be sprayed on the substrates and create defects.

3.5.2. Potential Source of Excess Metal 2: Contaminants in the Spray Chamber Atmosphere

Contamination from fibers and particles can occur from two primary sources. Firstly, contaminants floating in the atmosphere can get caught by the droplets during spray. The distance between the nozzle head and the substrate is approximately 3cm, but the wide spread of photoresist droplets increases the chance of contaminant entrapment. Secondly, the sprayed substrates are left inside the spray chamber for 5 minutes to be air-dried. This step was originally implemented to avoid insufficiently dried photoresist from flowing down as the substrates were placed in the oven at a 45 degree angle. During this process however, fibers and particles in the atmosphere can deposit on the wet photoresist surfaces and merge with the resist layer.

3.5.3. Potential Source of Excess Metal 3: Contaminants that Shadow UV during Imaging

There are a variety of contaminants in the atmosphere in the imaging area, including small white flakes that are consistently observed on the substrates. They can be easily removed with the nitrogen gas; however, they quickly redeposit on the photoresist surfaces in just a few minutes. If these particles are not fully removed from either the photoresist or the photomask surfaces during imaging, they could block the UV light and create a region of unexposed photoresist. The

unexposed areas of photoresist will not be developed away, and form excess metal defects by protecting the small area of metal underneath them from the etchants.

3.6. Potential Sources of Voids Defects through Insufficient Photoresist Strength and Coverage

Void defects are created when the etchants penetrate the photoresist layer and attack the metal layer. There are two fundamental causes by which the etchants penetrate the photoresist: imperfect photoresist coverage and insufficient photoresist strength. The following section describes these two causes and discusses the specific sources from which the imperfect coverage and insufficient strength could come from. Figure 3.13 summarizes these causes of void defects and the potential sources of photoresist defects.

3.6.1. Potential Source of Void 1: Too Large Droplets for the Thickness of the Photoresist

The current spray machine has an ultrasonic vibration nozzle frequency of 35kHz. According to Equation (1) and using physical properties of water as calculation basis (since the surface tension value of the custom photoresist mix is unknown), the droplet size corresponding to 35kHz frequency is 28.5 μm. Although 66% of the photoresist droplet is solvent that eventually evaporates, 28.5 μm droplet diameter can be too large for creating a 6.6 μm photoresist layer. When droplets are too large and not enough layers of these droplets are overlapping, they can fail to merge properly and form not only a rough uneven photoresist surface, but also small gaps in between the droplets. Etchants can penetrate through these small gaps and attack the metal layer to create voids. As a matter of fact, numerous vortex-like holes on the photoresist layer are visible when the substrates are viewed at an angle. Whether these vortexes reach all the way to the metal layer is unclear, but their presence confirms that the improper droplet merging is taking place.

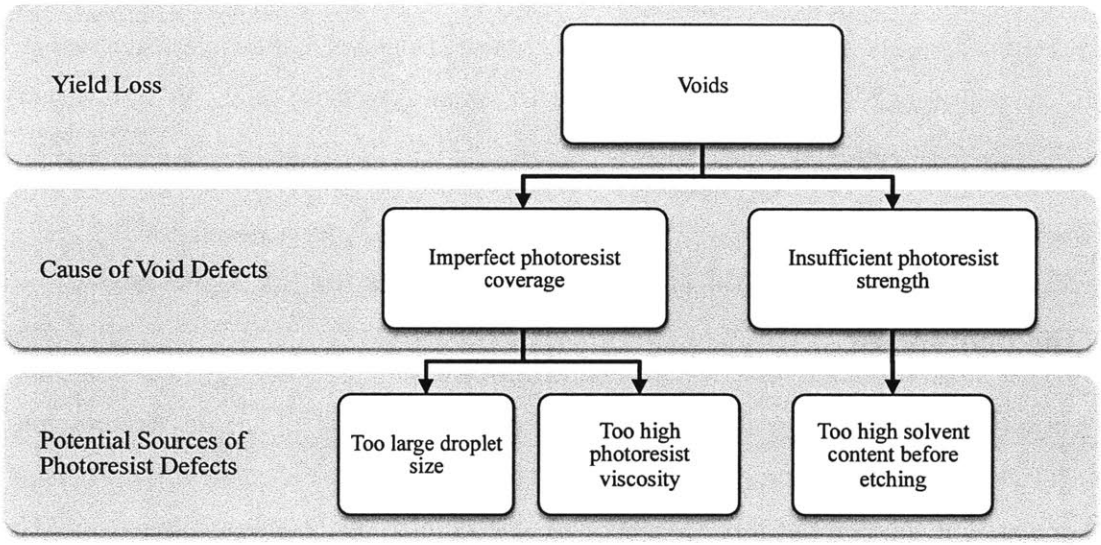

Figure 3.13: Summarized chart of sources of photoresist defects according to their respective causes of void defects.

3.6.2. Potential Source of Void 2: Too High Photoresist Viscosity

The current viscosity of the photoresist is 12.4 cSt with 22.5% solid content as shown in the calculations by Appendix 1. Given the extreme effect that solid content has on the roughness of the photoresist layer as shown in section 2.1.5, 22.5% solid content can be too high to achieve a smooth photoresist surface. When the solid content is high, the flowing effect is reduced and, therefore, the effective merging of the droplets is hindered. Similar to the consequences of too large droplets, high solid content level can aggravate the gap formation in between the droplets through which etchants can penetrate. A high flowing effect is especially important on high surface roughness materials such as the current PZT substrate, as the inherent substrate topology will be directly reflected on the photoresist layer if the droplets are not allowed to flow easily.

3.6.3. Potential Source of Void 3: Too High Solvent Content Before Etching

The photoresist layer can be insufficient in strength to fully withstand the chemically aggressive Ni and WTi etchant. The only step throughout the photolithography process that hardens the photoresist is the softbake process that reduces the solvent content of the photoresist down to 3~5%. Without any post image bake such as a hardbake process, the photoresist may contain too much solvent and become susceptible to the attack from the etchants. The effect of insufficient resist strength can be amplified if the photoresist surface is uneven. Uneven photoresist surfaces can have areas of thinner and, therefore, weaker photoresist, which will dissolve within the etchants faster.

CHAPTER 4

EXPERIMENTAL PROCEDURES

In order to determine the significance of each defect source, one experiment was designed and executed for each considered source of excess metal and voids. Comparison metric tests were first developed for excess metal and void defects and were conducted on standard substrates, the result of which served as the basis of comparison. The metric test was performed after each experiment to measure the difference in quality of the photoresist layer from the standard substrates. The following section discusses how each source was tested and how the metric tests were performed to compare the results of the tests.

4.1. Excess Metal Metric Test

The excess metal metric test was designed to generate a comparison metric for the subsequent excess metal experiments. The result of this test provided the total number of potential excess metal defects per substrate. This number was then used to determine and compare the ability of the experimental photoresist to reduce the number of excess metal. The photoresist-covered substrates were flood-exposed, developed then etched to see if any residue metal were present; the procedures were equivalent to that of the mapping test described in section 3.3. The excess

metal defects on the substrates were then marked and counted. This test was performed on 14 standard substrates and after the experiment outlined in Section 4.1. Figure 4.1 shows the process of excess metal metric test in chronological order.

4.2. Void Metric Test

The void metric test was also designed to provide a basis of comparison for the subsequent void experiments. The substrates covered with photoresist were carried through the standard imaging and etching process, but without the exposure process. The exposure step was removed from this experiment in order to maximize the number of voids, as patterning the photoresist removes the photoresist in the pattern areas and, therefore, reduces the total number of voids. However, the substrates were still submerged in the developer for 1 minute following the standard procedure, in order to include the effect of photoresist weakening through dark erosion in the test. If the photoresist is perfectly covering the metal layer and is of sufficient strength, no etchant molecules should be able to penetrate and affect the metal layer. The void defects are easily detected using a backlight as the light leaks through the voids in metal and can be marked for counting. The flow chart of void test is shown in Figure 4.2.

4.3. Excess Metal Effect Tests

One experiment was designed for each of the 3 sources of contamination: particles in the resist mix, particles in the atmosphere and particles shadowing during imaging. However, generating and maintaining a contaminant free atmosphere inside the spray chamber could not be completed with the available resources. The test required a customized positively pressurizing air handling unit, which was beyond the financial limitations of the project. Therefore, the effect of atmospheric contaminants was indirectly tested by controlling the other particle-contributing parameters. If controlling the other sources of contamination could not fully contain the photoresist contamination, it becomes highly likely that a significant portion of the contamination comes from the atmosphere. The pairing of the sources of excess metal and the corresponding effect experiment is summarized in Figure 4.3.

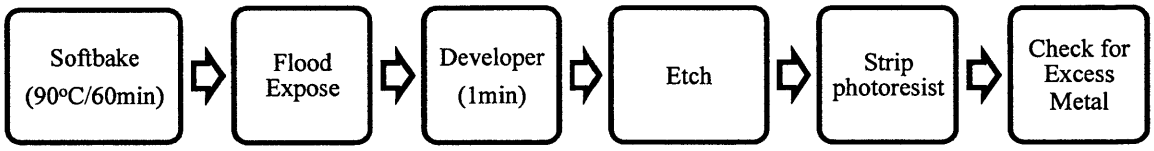

Figure 4.1: Flow chart of excess metal metric test.

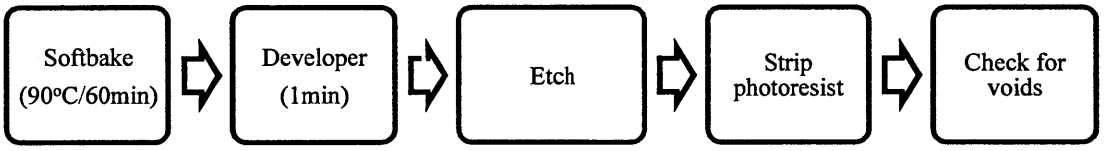

Figure 4.2: Flow chart of void metric test process.

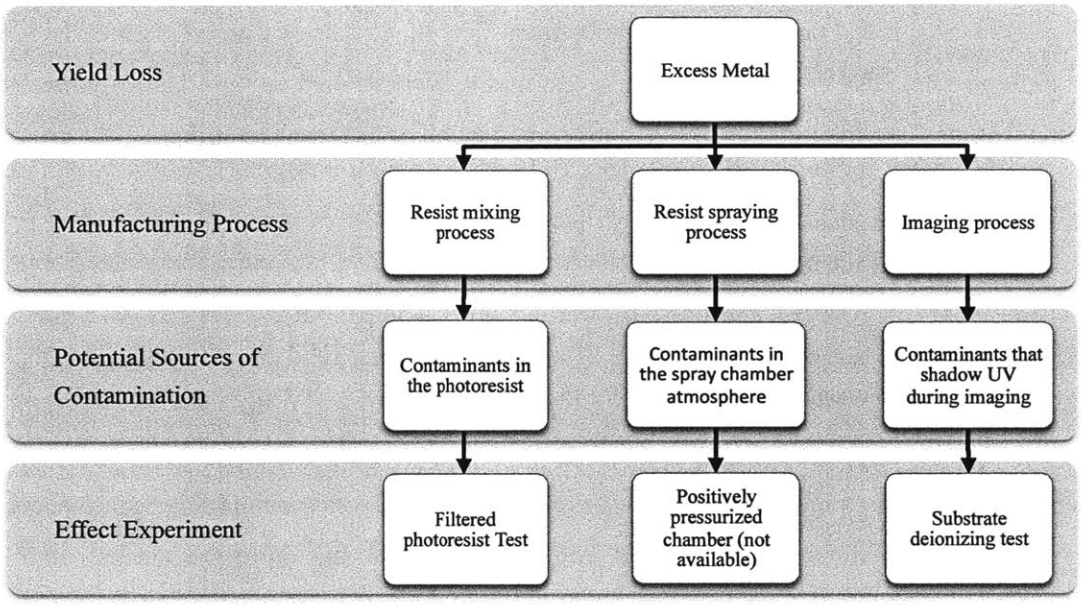

Figure 4.3: Summarized chart of sources of contamination and their corresponding effect experiments.

4.3.1. Filtered Photoresist Test

A filtered photoresist was used to test the effect of reducing the contaminants mixed in the photoresists on the number of excess metal defects. The photoresist syringe was first removed from the spray machine and replaced with a syringe containing pure solvent (PGMEA). The PGMEA solvent was injected into the system to rinse any residual photoresist from the tubes and the nozzle. A new quantity of photoresist was then passed through a 16 μm filter and injected into a clean syringe. The syringe containing the new filtered photoresist was loaded back into the machine and was sprayed normally onto 7 substrates. The flow chart of filtered photoresist test is shown in Figure 4.4. The excess metal metric test was then performed on the filtered-photoresist-covered substrates and the number of resultant excess metal defects was recorded.

4.3.2. Substrate Deionizing Test

A substrate deionizing test was designed to investigate the effect of reducing the surface contamination of the substrates or the masks that can shadow the UV light during exposure. In order to remove the static charge on the substrates that can accelerate the contaminant deposition, the substrates, as well as the carriers, were first blown with substrate deionizing for 10 seconds. The substrates were then placed on the aligner chuck and the substrate surface and the photomask were blown again for additional 10 seconds. Through the additional air blow, the contaminants on the affected areas were temporarily removed and, therefore, prevented from shadowing the UV light. The test was conducted on 16 work orders and the resultant average excess metal reject number was compared to that of the 2012 average. It must be noted that the work orders were processed all the way through to the inspection and not tested with excess metal metric tested due to the time limitation of running excess metal metric test on all 224 substrates. The flow chart of substrate deionizing test is shown in Figure 4.5.

4.4. Void Effect Tests

One test was designed for each of the three sources of voids in order to test their effect on the formation of void defects. The three sources were too thin photoresist for the droplet size, too

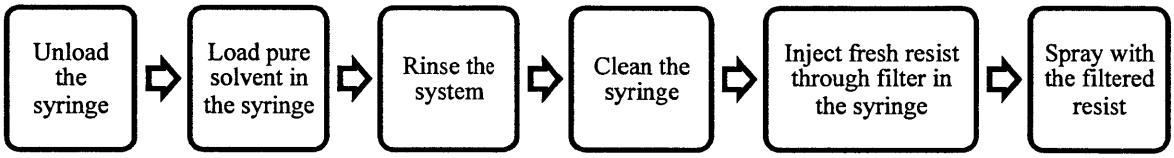

Figure 4.4: Flow chart of filtered photoresist test.

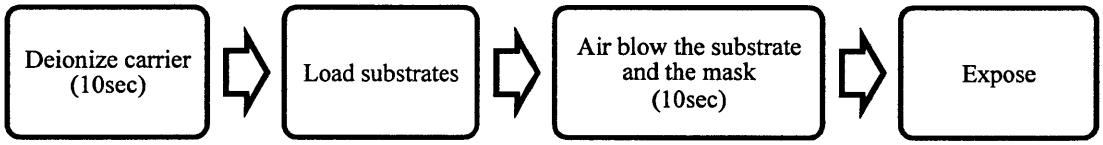

Figure 4.5: Flow chart of substrate deionizing test.

viscous photoresist and too high solvent content in the photoresist and their corresponding effect experiments are summarized in Figure 4.6.

4.4.1. Thicker Photoresist Test

A thicker photoresist test was performed to investigate the effect of reducing droplet size relative to the photoresist thickness. Reducing droplet size while maintaining the photoresist thickness will increase the number of droplet layers and, therefore, improve the droplet merging. Due to the constraints in resources, a new nozzle head could not be purchased to change the vibrating frequency and reduce droplet size. As a result, the resist thickness was increased instead so that the same effect of increased number of overlapping droplet layers could be simulated. The resist layer thickness was doubled from approximately 6.6 μm to 13.2 μm by reducing the scan speed by half, which will double the number of droplet layers and help the droplets merge better. The thicker photoresist however also gained in terms of the strength as the etchant will have to penetrate further in order to reach the metal layer. Therefore, in essence, the thicker photoresist test investigated the combined effect of increased coverage and strength. Seven of the double photoresist thickness substrates were tested with the void metric test and were compared to the result of the standard substrates. The flow chart of thicker photoresist test is shown in Figure 4.7.

4.4.2. Low Solid Content Resist Test

A low solid content test was performed in order to investigate the effect of lowering the solid content on the number of void defects. Lower solid content photoresist droplets will have a greater flowing effect and, therefore, form a smoother resist surface. The low solid content test started by first creating with a new photoresist that has 15% solid content instead of 22.5% then spraying it on regular substrates. The photoresist was mixed with a brand new set of chemicals in the same manner as the regular photoresist used by the company. 130.5 ml of the photoresist was mixed with 169.5 ml of PGMEA solution to create a 300 ml of 15% solid content photoresist. The scanning speed was also lowered to maintain the current photoresist thickness as more evaporation took place due to the higher solvent concentration. The void metric test was

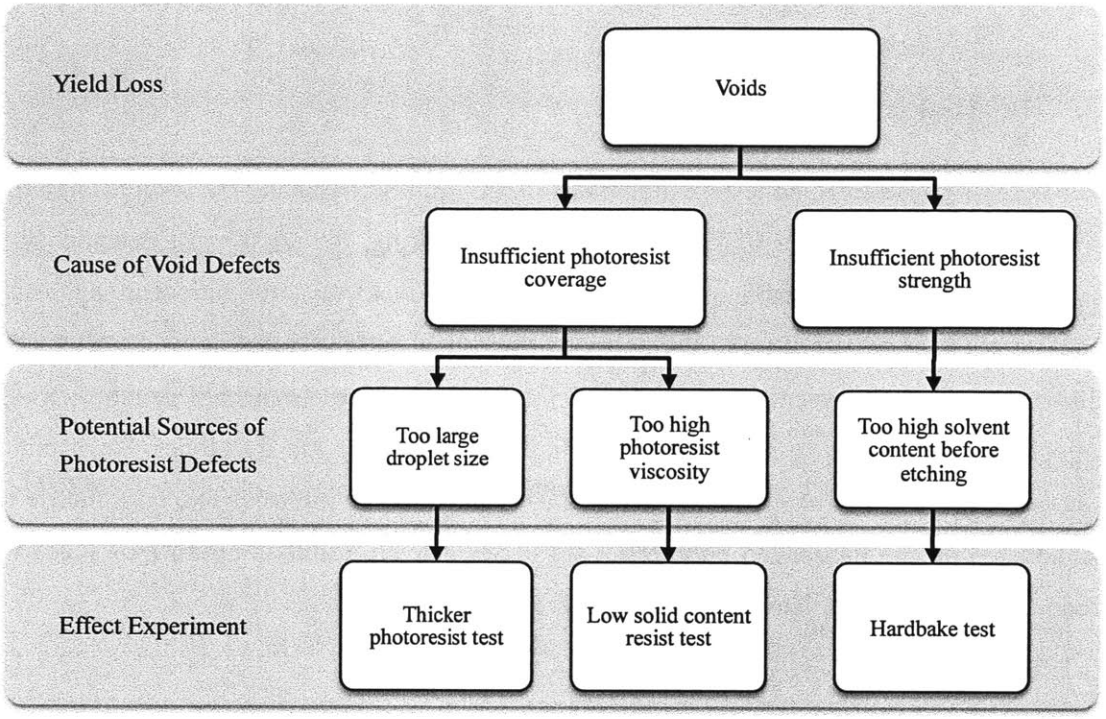

Figure 4.6: Breakdown of sources of void defect and their corresponding effect experiments.

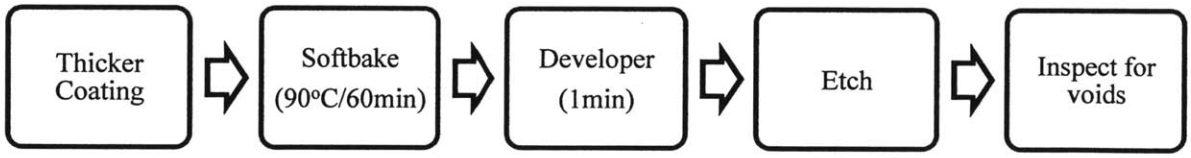

Figure 4.7: Flow chart of thicker photoresist test.

performed on seven of the smoother surface photoresist substrates and the resultant number of voids was recorded. The Figure 4.8 shows the chronological order of this test.

4.4.3. Hardbake Test

A hardbake test was performed to investigate the effect of further reducing the solvent content in the photoresist on the number of void defects. By hardbaking, the photoresist becomes more chemically and physically stable, which will allow the photoresist to withstand aggressive etchants for a longer period of time. Furthermore, the reflow and the rounding of the photoresist can also fill the gaps between the droplets and reduce the avenues of etchant penetration. The normal photoresist thickness substrates were first submerged in the developer for 1 minute without any exposure, and then were baked at 120°C oven for 20 minutes. The void metric test was conducted on the hardbaked photoresist substrates and the resultant number of voids was recorded. The flow chart of hardbake test is shown in Figure 4.9.

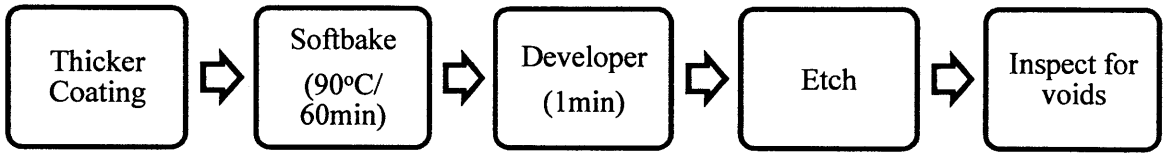

Figure 4.8: Flow chart of low solid content test.

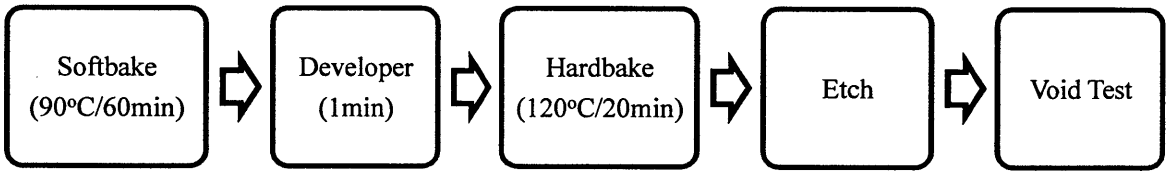

Figure 4.9: Flow chart of hardbake test.

CHAPTER 5

EXPERIMENTAL RESULTS

5.1. Excess Metal

The result of the each excess metal effect test was gathered and compared to the result of the excess metal metric test on the standard substrates. The two test results collectively suggest that excess metal primarily come from the contaminants in the photoresist and the spray chamber atmosphere. Usage of filtered photoresist helped reduce the photoresist contamination and decreased the substrate-wise excess metal occurrence to about half. However, some particle and fiber contamination was still observed in the photoresist layer even after the filtration, which suggests that additional contamination is taking place through the atmosphere during spray.

5.1.1. Excess Metal Metric Test on Standard Substrates

The result of the excess metal metric test on 14 standard substrates is shown in Table 5.1 and some of these resultant defects are illustrated in Figure 5.1 and Figure 5.2. The average number of excess metal, 5.5 was used as the basis of comparison for the rest of the excess metal tests. However, the resultant number of excess metal, as shown in Table 5.1, demonstrated a large

Table 5.1: Excess Metal Metric Test Result.

Substrates Number	Excess Metal Per Substrate
1	6
2	2
3	6
4	2
5	6
6	4
7	4
8	6
9	10
10	8
11	7
12	7
13	6
14	3
Average	**5.5**

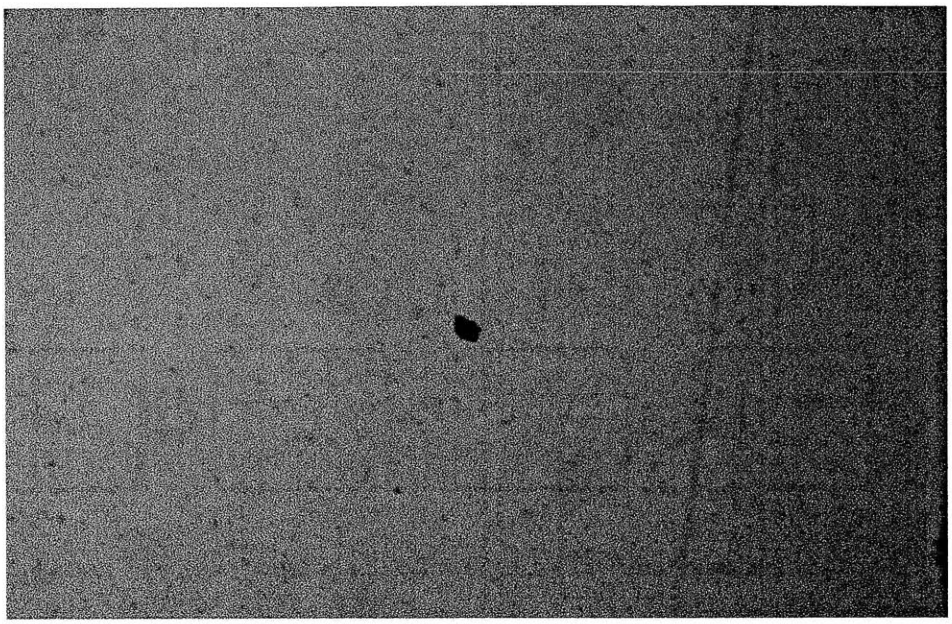

Figure 5.1: An example of a particle-induced excess metal from the excess metal metric test.

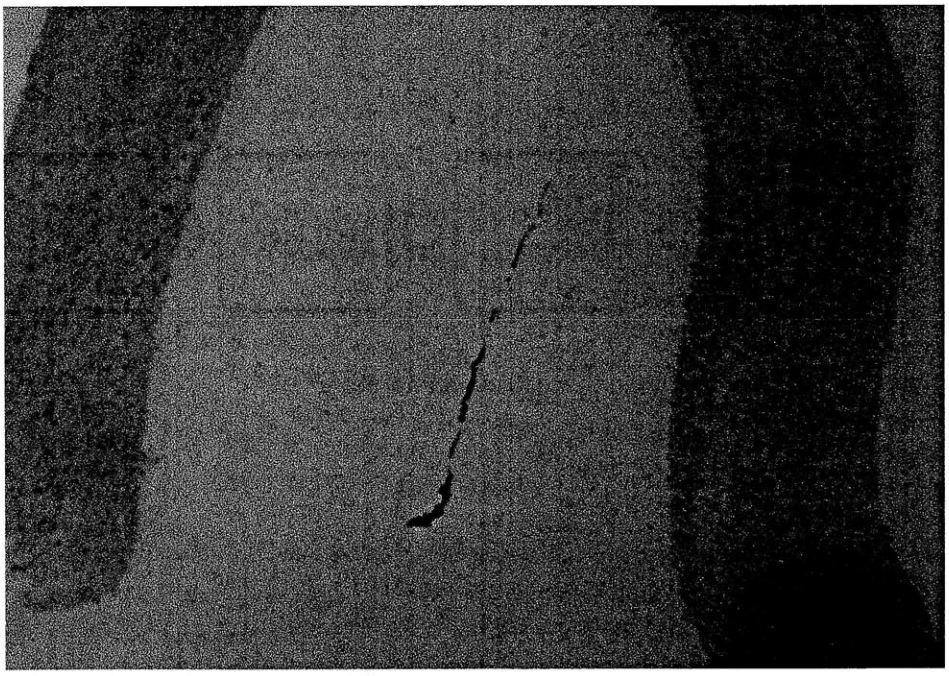

Figure 5.2: An example of a fiber-induced excess metal from the excess metal metric test result.

variation of the number of excess metal between the substrate, which may affect the accuracy of the result and the subsequent comparisons.

5.1.2. Filtered Photoresist Test

The result of the filtered photoresist test indicates that contaminants are mixed in the photoresist. Table 5.2 summarizes the result of the test on 7 substrates. It can be seen in Table 5 that the average was reduced to 2.1, about half the value of the metric 5.5. However, it must be noted that the experiment was conducted on only 7 substrates due to the limited resources, which reduces the reliability of the result.

Upon visual inspection of the photoresist before the metric test, it was observed that there is still contamination in the photoresist, although seemingly smaller in number. This suggests that the source of contamination is not solely the particles mixed in the photoresist, as the filtration process should have removed particles larger than 16 μm. Therefore, it was concluded that the contaminants in the spray chamber atmosphere got deposited on the wet photoresist during spraying and drying processes.

Furthermore, it was observed during the test that some of the particle defects were manifesting while the substrates were drying inside the chamber for 5 minutes. Within the first one or two minutes after the substrates were sprayed with the photoresist, contamination defects were appearing across the substrates. These defects were identifiable with naked eyes due to the characteristic bulging of the photoresist around the contaminants. It is possible that these contaminants were originally mixed in the photoresist but were becoming more visible as the solvent evaporated and the resist got thinner. However, assuming that the photoresist was properly filtered, it becomes more likely that the resist layers were being contaminated from the floating particles and fibers in the atmosphere.

5.1.3. Substrate Deionizing Test

The substrate deionizing test showed a small decrease in the number of rejected excess metal devices. The test was performed on 16 work orders to test for any reduction in excess metal

Table 5.2: Filtered photoresist test results.

	Excess Metal Per Substrate	
Substrates Number	Standard Procedures	With Filtered Resist
1	6	3
2	2	2
3	6	2
4	2	1
5	6	3
6	4	2
7	4	2
8	6	
9	10	
10	8	
11	7	
12	7	
13	6	
14	3	
Average	**5.5**	**2.1**

rejects and the result of the experiment is shown in Table 5.3. As can be seen in Table 5.3, there is a significant variation between the work orders, which can also be observed in standard production work orders. Although the average was slightly decreased from the 2012 average of 4.3 to 3.6, the wide distribution of the numbers make it difficult to establish a conclusion with certainty. The effect of eliminating static charges and surface contamination from shading UV light might be significant enough to lower the number of rejects, but a larger sample size test will be required to confirm the significance of this effect.

5.2. Voids

The result of the each void effect test was gathered and compared to the result of the void metric test. The three test results collectively indicate that the effects of both incomplete coverage of the photoresist and the insufficient strength are significant. The lower solid content test experimentally improved droplet merging and reduced void frequency by 47% and the hardbake test improved photoresist strength to reduce voids by 74%. The combined effect of the two, which was achieved by doubling the resist thickness, enabled almost complete removal of void defects.

5.2.1. Void Metric Test Result on Standard Substrates

The void metric test was conducted on 14 standard substrates to investigate how many potential voids a substrate is normally exposed. The test showed each substrate exhibits an average of 3.6 effective void defects and this number was used as the comparison metric for the following three void source tests. The result is summarized in Table 5.4 and some of the resultant voids are illustrated in Figure 5.3.

As the test was being conducted, it was noted that a significant portion of the voids was concentrated at the very edges of the substrate. It is likely that since the metal and the photoresist layers are thinner around the edges, metal around the edges are more susceptible to attacks from etchants. Furthermore, as these edges are removed and scrapped during dicing, a new metric

Table 5.3: Substrate deionizing test on 16 work orders and their excess metal defect number.

Work Order Number	Excess Metal Defects (out of 98 devices)
1	1
2	2
3	1
4	1
5	6
6	7
7	5
8	2
9	5
10	9
11	1
12	4
13	4
14	2
15	4
16	4
17	3
Average	**3.6**

Table 5.4: Void metric test on a regular softbake only substrates.

Regular Substrate (Softbake Only)		
Sub Number	Total Voids	Effective Voids
1	5	3
2	4	4
3	6	4
4	9	5
5	2	1
6	4	3
7	2	0
8	6	3
9	5	1
10	8	3
11	8	6
12	9	5
13	10	3
14	16	10
Average	**6.7**	**3.6**

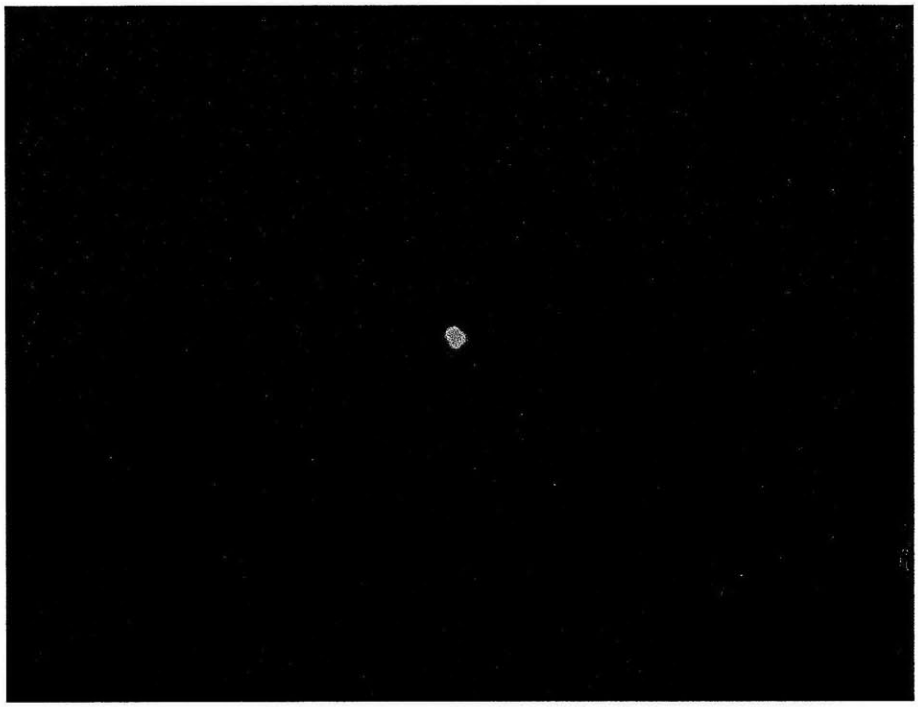

Figure 5.3: An example of void defect from the void metric test. The backlight shines through the void defect, which makes it easy to detect using a microscope.

"effective void" was introduced that represents only the number of voids that were inside the device regions. The effective void was considered as a more meaningful metric, therefore, was chosen as the standard of comparison.

5.2.2. Thicker Photoresist Test

The thicker photoresist test showed that increasing the strength and coverage removes the voids defects almost completely. The test was conducted on 7 substrates and the result is shown in Table 5.5. The test reduced the effective voids down to 0 and demonstrated the enhanced protective ability of the photoresist.

Upon visual inspection of the photoresist layer under a microscope, it was observed that there were no vortex shaped defects while they were present in the standard thickness or in the layers with 15% solid content. These results indicate that the increased number of droplet layers allow smooth merging of the droplets over the rough substrate surfaces and leave no gap for the etchants to penetrate.

5.2.3. Low Solid Content Photoresist Test

The low solid content photoresist test reduced the effective voids by 47%, from average 3.6 to 1.9 per substrate. The test was conducted on 14 substrates, which were sprayed with 15% solid content photoresist instead of the standard 22% solid content photoresist. The result of this test is summarized in Table 5.6. A wide variation in the values can be observed similar to the result of the metric test; however, the pattern of genuine reduction of voids can be detected.

Upon inspection of the photoresist prior to etching, it was observed that the vortex shaped figures in the substrates were still present. However, these vortexes did not look as large and as deep as those that are found in the standard photoresist layers. As a result, it was concluded that reducing the solid content of the photoresist droplets increased the flowing effect and, therefore, helped the droplets overcome the rough substrate surface and merge more effectively.

Table 5.5: Void test result of double thickness photoresist substrate.

	Regular Substrates		Double Thickness Photoresist	
Sub Number	Total Voids	Effective Voids	Total Voids	Effective Voids
1	5	3	1	0
2	4	4	0	0
3	6	4	0	0
4	9	5	0	0
5	2	1	1	0
6	4	3	0	0
7	2	0	0	0
8	6	3		
9	5	1		
10	8	3		
11	8	6		
12	9	5		
13	10	3		
14	16	10		
Average	**6.7**	**3.6**	**0.3**	**0**

Table 5.6: Low solid content photoresist test on 14 substrates.

	Regular Substrates		Lower Solid Content	
Sub Number	Total Voids	Effective Voids	Total Voids	Effective Voids
1	5	3	3	3
2	4	4	2	0
3	6	4	9	5
4	9	5	6	4
5	2	1	3	2
6	4	3	2	1
7	2	0	4	9
8	6	3	5	1
9	5	1	11	0
10	8	3	3	0
11	8	6	2	1
12	9	5	2	1
13	10	3	2	0
14	16	10	2	0
Average	**6.7**	**3.6**	**4.0**	**1.9**

5.2.4. Hardbake Test

The hardbake test revealed that increasing the strength of the photoresist layer by further reducing the solvent concentration improves the effective void count by 74%, from 3.6 to 0.9. The result of the void metric test on 13 hardbaked substrates is shown in Table 5.7. The voids that were observed in the hardbaked substrates appeared less frequently and were smaller in size. In fact, most of the voids found in this test were hardly detectable compared to those that are found in regular substrates. Therefore, it was concluded that hardbaking the substrates reduced the void defects by closing up some of the gaps in between droplets and increasing the photoresist's durability against the etchants.

In order to investigate at which temperature the thermal cross-linking occurs, the photoresist was also tested in two other temperature settings: 130 and 140°C. The thermal cross-linking began to occur at 140°C, due to which the photoresist required heated stripper for removal. Furthermore, the polarity and the capacitance of the devices were barely affected by these baking processes.

5.3. Summary of Results

A summary of the 2 excess metal experiments and 3 void experiments has been provided in Table 5.8. The results are represented by the percentage reduction that each test attained respective to its comparison metric. As table 5.8 shows, the filtered photoresist test was compared to the excess metal metric test of standard substrates, the substrate deionizing test was compared to the 2012 average excess metal rejects, and all of the void tests were compared to the void metric test of standard substrates.

Table 5.7: Hardbaked photoresist test on 13 substrates.

	Regular Softbaked Substrates		Hardbaked Substrates	
Sub Number	Total Voids	Effective Voids	Total Voids	Effective Voids
1	5	3	1	0
2	4	4	0	0
3	6	4	1	0
4	9	5	4	0
5	2	1	1	0
6	4	3	2	2
7	2	0	3	1
8	6	3	4	2
9	5	1	0	0
10	8	3	2	2
11	8	6	4	2
12	9	5	2	0
13	10	3	5	3
14	16	10		
Average	**6.7**	**3.6**	**2.2**	**0.9**

Table 5.8: The summary table of all results. The results are represented in the percentage reduction relative to their respective comparison metric.

Excess Metal Tests	Result from Standard Substrate	Result from the test	Percentage Reduction (%)
Filtered Photoresist Test	5.5 (defect/substrate)	2.1	62
Substrate Deionizing Test	4.3 (reject/work order)	3.6	16
Void Tests			Percentage Reduction (%)
Thicker Photoresist Test	6.7 (defect/substrate)	0	100
Low Solid Content Test	6.7 (defect/substrate)	3.6	47
Hardbake Test	6.7 (defect/substrate)	1.9	75

CHAPTER 6

CONCLUSIONS

6.1. Excess Metal Test Conclusions

The two excess metal defect tests showed that the effect of contamination through mixing, and the spray chamber atmosphere are the most significant. The filtered photoresist test confirmed that some of the contamination is happening as early as during the mixing process of the photoresist while the rest of the contaminants are coming from the spray chamber atmosphere. Therefore, it is important that the photoresist is free of contamination and not stored at the room temperature for long while the spray chamber stays clean.

First, a filtration step for the photoresist can be implemented. The filter can be placed inside the spray system, through which all photoresist is pressurized through an interchangeable filter, or the photoresist can be separately filtered before being loaded into the machine. These filters will remove the contaminants that are mixed in the photoresist.

Additionally, the size of the photoresist reservoir in the spray machine can be reduced. Sometimes there is enough photoresist for one month of operation inside the spray machine; one month is more than enough for room-temperature and high-solvent photoresist to develop

precipitates. The exact number of days before which the photoresist remains free of precipitants will need to be experimentally verified.

Furthermore, the spray chamber can be positively pressurized. A positively pressurized chamber will keep any outside contamination from entering and depositing on the substrates given that the inside cleanliness of the chamber is maintained. It must be noted that positive pressure should not generate a strong enough airflow to affect the spread of the photoresist drop.

Finally, the spray chamber must be more frequently and regularly cleaned. Currently, the cleaning schedule is not regular and the chambers are often cleaned during the spray machine idle days. Cleaning that is conducted 12 to 24 hours prior to spraying greatly loses its effectiveness, as contaminants will rapidly reenter the chamber. Hence, a strict cleaning routine must be enforced, which takes place just before the spraying operation begins.

6.2. Void Test Conclusions

The results of the three void defect tests showed that insufficient photoresist coverage and the chemical durability are working together to create void defects in the final devices. Therefore, it is important that a smoother surface with an increased strength photoresist layer is utilized in the photolithography process.

First, a lower solid content photoresist can be used. The current photoresist is too viscous for the droplets to flow and merge effectively and, therefore, areas of weak or no photoresist are developing. This effect is amplified by the rough surface of the current substrates and, therefore, it is critical to allow the droplets to spread more fluently.

Furthermore, a smaller droplet size can be utilized. A new nozzle head that vibrates in a higher frequency such as 120 kHz or 130 kHz will reduce the droplet size from 29 μm down to 12 μm. With the droplet size of 12 μm, the photoresist droplets will stack with approximately twice the number of layers in order to create the same total thickness. This will ensure that the photoresist layer becomes more even and the gaps between the droplets are properly filled.

Thirdly, a hardbake process can be implemented. Areas of weak photoresist can be reinforced by a hardbake process and the reflow effect of photoresist can help the photoresist layer become more even.

CHAPTER 7

RECOMMENDED FUTURE WORK

The experiments that were conducted during the course of this thesis did not include advanced statistical verification; hence, further analyses in larger scale are recommended. This section will discuss the future experimentations that could be conducted to better confirm the result and the conclusion of this thesis.

6.3. Larger Scale Experiments

All experiments need to be conducted in a larger scale, for both excess metal and void defects. The variation between the work orders and substrates are too large that a small improvement cannot be detected with a reasonable level of confidence with a small sample size. Hence, a larger quantity of data must be harvested in order to yield a more conclusive result.

6.4. Shorter Softbake

The effect of shorter softbake process can be investigated. The current softbake, 90°C for 60 minutes, might be too long. As established by the hardbake test, the current softbake is not

sufficiently strong enough to perfectly withstand the etchant. However, it might also be too strong for the imaging process and leave residues, which could lead to excess metal. Therefore, substrates baked at a short period of time such as 50 and 40 minutes can be tested for substrate-wise excess metal counts.

6.5. Particles on the Substrates

Although the substrates are cleaned with alcohol and sprayed with deionizing air before being placed onto the spray plate, it might not be sufficient to remove all the particles that accumulate on the PZT surface. Some particles and fibers are resilient to a certain degree to the nitrogen spray and could be processed with the substrates unnoticed. Furthermore, there tends to be a long gap of usually 24 hours in between the alcohol cleaning step and the photoresist spraying step, during which the substrates could be contaminated.

6.6. Chemical Analysis

A chemical analysis on the most common particles and the fibers can be conducted in order to determine the chemical composition and find out their sources. If the sources of these particles and fibers are can be identified, additional changes could be made to reduce the particle generation.

CHAPTER 7

APPENDIX: PHOTORESIST VISCOSITY

The current viscosity of the photoresist mixture was first investigated and compared to the literature-recommended viscosity of 5cSt. Refutas equation was used to calculate the viscosity of two liquid mixtures, using a property called Viscosity Blending Index (VBI, also called as Viscosity Blending Number). The first step is to compute the VBI of each liquid [13].

$$\mathrm{VBI} = 14.534 \times \ln[\ln(\upsilon + 0.8)] + 10.975 \tag{A1}$$

where υ is the kinetic viscosity of the liquid. Once the VBIs are calculated, they are multiplied by the mass fraction x_n then summed.

$$\mathrm{VBI_{Blend}} = (x_A)(\mathrm{VBN_A}) + (x_B)(\mathrm{VBN_B}) + \cdots + (x_N)(\mathrm{VBN_N}) \tag{A2}$$

The final VBI of the blend liquid is then used in the reorganized Equation (A1) to yield the final viscosity as:

$$\upsilon = \exp\left(\exp\left(\frac{\mathrm{VBI_{Blend}} - 10.975}{14.534}\right)\right) - 0.8 \tag{A3}$$

The current photoresist is mixed in the solvent to photoresist volumetric ratio of 1 to 2. This ratio was first converted into a mass ratio based on its density, after which the VBI calculation was performed as shown in Table 2.

Table 7.1: VBI calculation for the current resist.

Material Properties				
	Viscosity (cSt)	Density (g/cm3)	Weight Ratio (%)	Solid Content (%)
Solvent	1.1	0.959	0.312	0
Photoresist	127	1.055	0.688	32.7

VBI Calculations				
	VBI	VBI-Blend	Final Viscosity	Final Solid Content
Solvent	4.53	24.74	12.37	22.48
Photoresist	33.93			

REFERENCES

1. Dave, N., 2012, "Identification and removal of metal oxide defects through improved semi-anisotropic wet etching process" Master's thesis, MIT, Cambridge, MA.
2. Alsaeed, A., 2012, "Elimination of PZT Thin Film Breakage Caused By Electric Current Arcing and Intrinsic Differential Stains During Poling" Master's thesis, MIT, Cambridge, MA.
3. Pham, N.P., Scholtes, T.L., Klerk, R., Wieder, B., Sarro P.M. and Burghartz, J.N., 2001, "Direct spray coating of photoresist for MEMS applications," *Micromachining and Microfabrication Process Technology VII,* **4557**., pp.154-158
4. MicroChemicals, 2009, "Spray Coating of Photoresist.", from http://www.microchemicals.com/technical_information/spray_coating_photoresist.pdf.
5. MicroChemicals, 2009, "Photoresist Coating Techniques.", from http://www.microchemicals.com/technical_information/photoresist_coating.pdf.
6. Sonaer Ultrasonics, 2012, "Ultrasonic Atomizer Nozzles for Making Fine Particles from Liquids.", from http://sonozap.com/Atomizer_Nozzles.html
7. Lang, R.J., 1962 "Ultrasonic Atomization of Liquids." The Journal of the Acoustical Society of America, 34.1., pp. 6-8.
8. MicroChemicals, 2010, "Exposure of Photoresists.", from http://www.microchemicals.com/technical_information/exposure_photoresist.pdf.
9. Barron, A.R., 2009, "Composition and Photochemical Mechanisms of Photoresists." Creative Commons, 1.2., pp. 1-7
10. MicroChemicals, 2007, "Softbake of Photoresist Films." from http://www.microchemicals.com/technical_information/softbake_photoresist.pdf.
11. MicroChemicals, 2010, "Hardbake of Photoresist Structures." from http://www.microchemicals.com/technical_information/hardbake_photoresist.pdf.
12. MicroChemicals, 2010, "Reflow of Photoresist.", from http://www.microchemicals.com/technical_information/reflow_photoresist.pdf
13. Robert E. Maples, 2000, *Petroleum Refinery Process Economics*, 2nd ed., Pennwell Books.